

This is a repository copy of Effect of Ca(OH)2 on the immobilization of simulated radioactive borate waste in metakaolin-based geopolymer waste forms.

White Rose Research Online URL for this paper: <a href="https://eprints.whiterose.ac.uk/id/eprint/232885/">https://eprints.whiterose.ac.uk/id/eprint/232885/</a>

Version: Accepted Version

#### Article:

Kim, B., Walkley, B. orcid.org/0000-0003-1069-1362, Provis, J.L. et al. (2 more authors) (2025) Effect of Ca(OH)2 on the immobilization of simulated radioactive borate waste in metakaolin-based geopolymer waste forms. Cement and Concrete Research, 197. 107946. ISSN: 0008-8846

https://doi.org/10.1016/j.cemconres.2025.107946

© 2025 The Authors. Except as otherwise noted, this author-accepted version of a journal article published in Cement and Concrete Research is made available via the University of Sheffield Research Publications and Copyright Policy under the terms of the Creative Commons Attribution 4.0 International License (CC-BY 4.0), which permits unrestricted use, distribution and reproduction in any medium, provided the original work is properly cited. To view a copy of this licence, visit http://creativecommons.org/licenses/by/4.0/

#### Reuse

This article is distributed under the terms of the Creative Commons Attribution (CC BY) licence. This licence allows you to distribute, remix, tweak, and build upon the work, even commercially, as long as you credit the authors for the original work. More information and the full terms of the licence here: https://creativecommons.org/licenses/

#### Takedown

If you consider content in White Rose Research Online to be in breach of UK law, please notify us by emailing eprints@whiterose.ac.uk including the URL of the record and the reason for the withdrawal request.



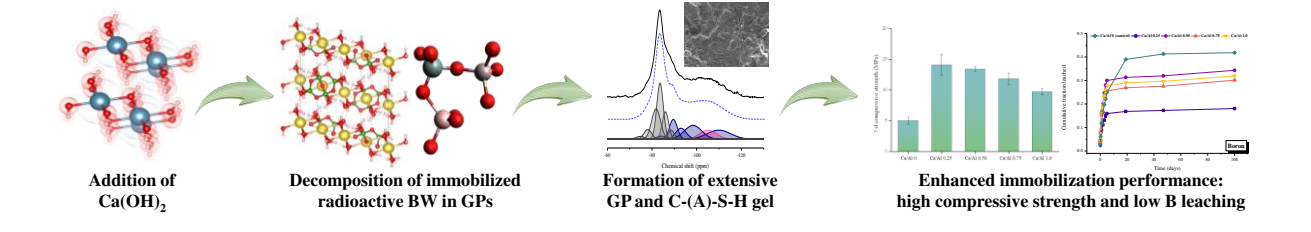
# **Cement and Concrete Research**

# Effect of calcium on the immobilization of simulated radioactive borate waste in metakaolin-based geopolymer waste forms --Manuscript Draft--

Manuscript Number:	CEMCON-D-25-00262					
Article Type:	Research paper					
Keywords:	Geopolymer waste form, Radioactive borate waste, Cumulative fraction leached, Immobilization, Calcium hydroxide					
Corresponding Author:	Byoungkwan Kim, Ph.D., Pohang University of Science and Technology KOREA, REPUBLIC OF					
First Author:	Byoungkwan Kim, Ph.D.,					
Order of Authors:	Byoungkwan Kim, Ph.D.,					
	Brant Walkley					
	John L Provis					
	Hyun-min Ma					
	Wooyong Um					
Abstract:	Geopolymers are promising candidates for immobilizing radioactive borate waste (BW) but their performance needs improvement as borate negatively affects their physicochemical properties. This study investigated the effect of Ca(OH) <sub>2</sub> on geopolymer waste forms by varying the Ca/Al ratio (0.25-1.0). At a Ca/Al ratio of 0.25, Ca(OH) <sub>2</sub> tripled the compressive strength (5 to 14 MPa) by promoting geopolymerization reaction and forming C-(A)-S-H gel. The increased pH and the reactive Ca led to the decomposition of immobilized BW. A low Ca/Al ratio caused minimal structural changes, while higher ratios promoted C-(A)-S-H gel formation. Characterization results confirmed the formation of extensive geopolymers and a compact microstructure. Notably, the cumulative fraction leached of B decreased more than twofold, and the leachability index increased from 7.5 to 8.7. This research provides insights into the role of calcium in immobilizing radioactive BW in geopolymers, emphasizing the importance of optimizing the Ca/Al ratio to enhance immobilization performance.					
Opposed Reviewers:						

# Highlights

- Presence of Ca(OH)<sub>2</sub> at least doubles the compressive strength.
- Ca(OH)<sub>2</sub> addition promotes geopolymerization and formation of the C-(A)-S-H gel.
- Ca(OH)<sub>2</sub> reduced the leaching of B by up to 57%.
- Physically or chemically immobilized BW was decomposed by Ca(OH)<sub>2</sub> addition.



# 1 Effect of calcium on the immobilization of simulated radioactive borate

- 2 waste in metakaolin-based geopolymer waste forms
- 3
- 4 Byoungkwan Kim<sup>a, b,\*</sup>, Brant Walkley<sup>b</sup>, John L Provis<sup>c</sup>, Hyun-min Ma<sup>a</sup>, and Wooyong Um<sup>a, d, e, \*</sup>
- 5
- <sup>a</sup> Division of Advanced Nuclear Engineering (DANE), Pohang University of Science and
- 7 Technology (POSTECH),77 Cheongam-Ro, Nam-Gu, Pohang, Gyeongbuk, Republic of Korea
- 8 b School of Chemical, Materials and Biological Engineering, The University of Sheffield, S1
- 9 3JD, United Kingdom
- <sup>c</sup> Laboratory for Waste Management (LES), Paul Scherrer Institut, Forschungsstrasse 111,
- 11 5232 Villigen PSI, Switzerland.
- d Division of Environmental Science and Engineering (DESE), Pohang University of Science
- and Technology (POSTECH), 77 Cheongam-Ro, Nam-Gu, Pohang, Gyeongbuk, Republic of
- 14 Korea
- 15 e Nuclear Environmental Technology Institute (NETI), Pohang University of Science and
- 16 Technology (POSTECH), 77 Cheongam-Ro, Nam-Gu, Pohang, Gyeongbuk, Republic of
- 17 Korea
- 18
- 19 \* Co-corresponding authors:
- 20 B. Kim, kwan928@postech.ac.kr, Tel.:+82-54-279-9568, Fax:82-54-279-9559
- 21 W. Um, wooyongum@postech.ac.kr, Tel.:+82-54-279-9563, Fax:+82-54-279-9559
- 23

22

#### **Abstract**

Geopolymers are promising candidates for immobilizing radioactive borate waste (BW), but their performance needs improvement as borate negatively affects their physicochemical properties. This study investigated the effect of Ca(OH)<sub>2</sub> on geopolymer waste forms by varying the Ca/Al ratio (0.25-1.0). At a Ca/Al ratio of 0.25, Ca(OH)<sub>2</sub> tripled the compressive strength (5 to 14 MPa) by promoting geopolymerization reaction and forming C-(A)-S-H gel. The increased pH and the reactive Ca led to the decomposition of immobilized BW. A low Ca/Al ratio caused minimal structural changes, while higher ratios promoted C-(A)-S-H gel formation. Characterization results confirmed the formation of extensive geopolymers and a compact microstructure. Notably, the cumulative fraction leached of B decreased more than twofold, and the leachability index increased from 7.5 to 8.7. This research provides insights into the role of calcium in immobilizing radioactive BW in geopolymers, emphasizing the importance of optimizing the Ca/Al ratio to enhance immobilization performance.

- 40 Keywords: Geopolymer waste form, Radioactive borate waste, Cumulative fraction
- 41 leached, Immobilization, Calcium hydroxide

#### 1. Introduction

Neutron-absorber materials, such as H<sub>3</sub>BO<sub>3</sub>, are commonly used in the operation of pressurized water reactors, which generate a large quantities of boron (B)-containing liquid

radioactive waste [1]. This radioactive liquid waste is subjected to concentration and drying processes to reduce its volume [2]. The dried and concentrated waste (borate waste; BW) consists of B<sub>2</sub>O<sub>3</sub> (63%), H<sub>2</sub>O (26%), and Na<sub>2</sub>O (10%) [1, 2] and it is categorized as low and intermediate-level radioactive waste (LILW) under South Korea's radioactive waste classification. Hence, radioactive BW should be immobilized in a waste form to address environmental concerns. The disposal of LILW such as BW and ion exchange resins in South Korea has become a critical issue due to the absence of a suitable waste form matrix for solidification/stabilization [3]. Approximately 20,015 drums of low-level radioactive waste (BW), each with a volume of 200 L, are temporarily retained at nuclear power plant facilities [4].

Ordinary Portland cement (OPC) is commonly used for making a cement waste form to immobilize LILW due to its cost-effectiveness, simple fabrication, and good durability [5-7]. However, cement waste forms are unsuitable for immobilizing radioactive BW because of the interaction between calcium compound and borate. This chemical reaction forms insoluble calcium borate hydrated phases on the cement particles [8], which impedes the hydration reaction and adversely affects the physical properties of the cement waste form, such as delaying setting, lowering waste loading, and lowering the compressive strength [8-10]. Calcium sulfoaluminate cement has been proposed as an alternative to OPC; however, it also experiences setting retardation due to the formation of semi-crystalline or amorphous calcium borate phases [11]. In addition, glass waste form and organic waste form such as polymer and paraffin wax have been proposed as alternatives [1, 2, 12]. The glass waste form can effectively immobilize radionuclides by incorporating an amorphous structure through vitrification [13]. However, the associated glass fabrication costs are substantial and the high-temperature

process (exceeding 1000 °C) necessitates special facilities. Even though organic waste forms can achieve higher waste loading than cement waste forms, but poor leaching resistance and layer separation by polarity difference, among other problems, have been reported [12].

Geopolymers have a three-dimensional amorphous aluminosilicate nanostructure and are now widely investigated to immobilize various radionuclides and radioactive wastes. Geopolymers are formed by a polycondensation reaction of alkaline activators and amorphous aluminosilicate substances such as metakaolin and fly ash [14]. Geopolymers are characterized by a three-dimensional aluminosilicate framework nanostructure, in which Al substitutes for some of the Si tetrahedra and the charge deficiency is balanced by alkali cations [14]. As a result, the aluminosilicate framework in geopolymers has a permanently negative charge and cationic radionuclides such as Cs, Co, and Sr can be encapsulated more within the geopolymer nanostructure through electrostatic forces [15]. These properties have been exploited to immobilize various radioactive wastes such as Cs-loaded chabazite [16], spent ion-exchange resin [17, 18], waste oil [19, 20], spent liquid scintillation cocktail [21, 22], and Cs-contaminated soil [23], using geopolymer waste forms.

However, immobilizing radioactive waste containing B in geopolymers is challenging, as B reacts with Si to form B-O-Si networks. This leads to delayed setting and a decrease in compressive strength [24]. In our previous study, we investigated the optimal Si/Al ratio and curing conditions for immobilizing BW using geopolymers [25]. The Si/Al ratio of 1.4 was found to be favorable and curing for 1 d at room temperature and 6 d at 60 °C resulted in a high waste loading of 30 wt% [25]. The fabricated geopolymer waste forms met the compressive strength criterion (>3.45 MPa) after undergoing waste acceptance criteria tests for South Korea such as <sup>60</sup>Co γ-ray irradiation, 90-day long-term immersion, and thermal cycling test. In

addition, the average leachability index after a 90-day long-term leaching test was 7.5, and the leaching mechanism of B was governed by diffusion [25]. Overall, the geopolymer waste form achieved three times higher waste loading and excellent durability compared to cement; however, the compressive strength only marginally met the criterion (3.445 MPa) [25]. Therefore, approaches to enhance the durability of geopolymer incorporating BW are needed. A common method of accelerating the reaction kinetics of geopolymers and improving their mechanical properties is adding calcium sources such as calcium hydroxide (Ca(OH)<sub>2</sub>), gypsum, or blast furnace slag. Considering the limited supply of blast furnace slag and the weakly basic properties of gypsum, Ca(OH)<sub>2</sub> emerges as a highly favorable additive [26]. The incoporation of Ca(OH)2 enhances the dissolution rate of raw materials and accelerates the setting of geopolymer [27, 28]. It also leads to the development of a Ca-rich gel like calcium (aluminum) silicate hydrate (C-(A)-S-H) gel which contributes to the densification of the structure and, thus improvements in the compressive strength [28]. Therefore, in this study, Ca(OH)<sub>2</sub> was added to metakaolin-based geopolymer waste form containing BW to evaluate its potential as a mineral additive for enhancing the physicochemical properties and leaching stability of geopolymer waste form. The Ca/Al ratio in the reaction mixture was incrementally varied to understand the structural changes induced by Ca(OH)<sub>2</sub> and determine the optimal amount of Ca(OH)2 addition. The resulting effects on mechanical strength, micro- and nanostructure, BW immobilization mechanism, and B leaching behavior in geopolymer waste forms were then examined.

113

114

115

93

94

95

96

97

98

99

100

101

102

103

104

105

106

107

108

109

110

111

112

#### 2. Materials and method

#### 2.1 Fabrication of simulated radioactive BW and geopolymer waste form

Reagent grade commercial chemicals, such as sodium tetraborate decahydrate (borax, Na<sub>2</sub>B<sub>4</sub>O<sub>7</sub>·10H<sub>2</sub>O), and K, Na, Zn, Ca, and Mg nitrate salts (KNO<sub>3</sub>, NaNO<sub>3</sub>, Zn(NO<sub>3</sub>)<sub>2</sub>·6H<sub>2</sub>O, Ca(NO<sub>3</sub>)<sub>2</sub>·4H<sub>2</sub>O, and Mg(NO<sub>3</sub>)<sub>2</sub>·6H<sub>2</sub>O) were used to prepare simulated radioactive BW. They were dissolved in 1000 mL of deionized water (DIW) to achieve the chemical composition listed in Table 1 [10]. The detailed chemical information for simulanted radioactive BW was provided by Korea Hydro & Nuclear Power Co., Ltd. The mixture was dried at 105 °C for 1 d and then crushed to powder (<75 μm) using a small grinder. Table 1. Chemical composition of simulant radioactive BW [10]

Table 1. Chemical composition of simulant radioactrive BW [10]

Element	В	Na	K	Ca	Zn	Mg
Concentration (ppm)	221,490	76,000	2,333	1,600	583	495

High-purity commercial metakaolin (SiO<sub>2</sub> 51.1% and Al<sub>2</sub>O<sub>3</sub> 43.9%), potassium hydroxide solution (K<sub>2</sub>O 45%), potassium silicate solution (K<sub>2</sub>O 22% and SiO<sub>2</sub> 28%), calcium hydroxide (Ca(OH)<sub>e</sub>, assay 95%) were used as starting materials for preparing the geopolymer waste form. The metakaolin-based geopolymer waste forms were formulated by mixing an alkaline activator with Ca(OH)<sub>2</sub> and metakaolin to obtain a stoichiometry of xCaO·K<sub>2</sub>O·Al<sub>2</sub>O<sub>3</sub>·2.8SiO<sub>2</sub>·10H<sub>2</sub>O (x = 0.25, 0.50, 0.75, and 1.00) (Table 2). The waste loading of simulated radioactive BW was maintained at 30 wt% (Table 2), which is the maximum waste loading for metakaolin-based geopolymer waste forms, as based on our previous study [25]. This molar ratio was chosen based on previous studies to achieve high durability and high waste loading [25]. The prepared alkaline activator, metakaolin, Ca(OH)<sub>2</sub>, and BW were mixed in a high-shear planetary mixer at 1400 RPM for 4 min and then degassed at 2100 RPM for 30

s. The fresh geopolymer paste was poured and sealed in cylindrical molds ( $\emptyset$  30 mm and H 60 mm). The trapped air voids were removed using a vibrator for 30 s. All geopolymer waste forms were cured at  $26 \pm 1$  °C and 60 °C for 6 d according to the optimized curing conditions [25].

Table 2. Formulation condition of geopolymer waste forms [25]

Si/Al	K/A1	H <sub>2</sub> O/Al	Ca/Al	BW content (wt%)	Curing
1.4	1.0	10.0	0.25 0.50 0.75 1.00	30%	26 ± 1 °C for 1d + 60 °C for 6d

# 

#### 2.2 Characterizations

### 2.2.1 Compressive strength

The compressive strength of each geopolymer waste form was measured after 7 d of curing. Three samples of each mix formulation were tested using a compression testing machine (Salt Co Ltd., ST-1001) at a loading rate of 0.6 MPa/s, in accordance with the Korean standard test method (KS F 2405).

### 2.2.2 X-ray diffraction (XRD)

X-ray diffraction patterns were collected to investigate the mineralogical properties of geopolymer waste form X-ray diffractometer (Rigaku, MiniFlex, Japan) and running at 40 kV and 15 mA (Cu K radiation). The step size for was  $0.02^{\circ}$ , and the scan speed was  $1^{\circ}$ /min. The data ranged from  $5^{\circ}$  to  $65^{\circ}$  2  $\theta$ . The search and match program (PDXL) and crystal information databased (PDF-2 release 2021) were used to identify the crystalline phases.

#### 2.2.3 Solid-state magic angle spinning nuclear magnetic resonance (MAS NMR)

<sup>29</sup>Si magic angle spinning (MAS) nuclear magnetic resonance (NMR) spectra were obtained using a 400 MHz solid-state MAS NMR AVANCE III HD spectrometer (Bruker, Germany). A 4 mm zirconia rotor and a HX-MAS probe were used. The pulse width of the NMR spectra was 1.5 s at 79.495 MHz. The spinning frequency was 11 kHz, and the recycle time was 20 s. The total scan number was 3000. Peakfit software was used to fit Gaussian distributions to deconvolute the overlapping resonance peaks.

The 600 MHz solid-state Unity-Inova NMR spectrometer (14.1 T, Agilent Technologies, USA) equipped with a 2.5 mm zirconia rotor and CPMAS DR probe were used for <sup>11</sup>B and <sup>27</sup>Al MAS NMR analysis. The Larmor frequency for <sup>11</sup>B and <sup>27</sup>Al was 192.546 and 156.335 MHz, respectively. The spinning speed, pulse length, relaxation time, and scan number for <sup>11</sup>B MAS NMR analysis were 23 kHz, 1.1 s, 2 s, and 512, respectively. The <sup>27</sup>Al MAS NMR spectra were collected with a pulse length of 0.8 s and a relaxation latency of 2 s. The spinning frequency was 22 kHz, and the scan number was 1024.

 $^{23}$ Na MAS NMR spectra were obtained using a Bruker Avance III HD 500 spectrometer at 11.7 T with a 4.0 mm dual resonance CP/MAS probe, yielding a Larmor frequency of 132.29 MHz for  $^{23}$ Na. The spectra of  $^{23}$ Na MAS were acquired using a 3 μs non-selective ( $\pi$ /2) excitation pulse, a measured 10 s relaxation delay, a total of 128 scans and spinning at 12.5 kHz. All  $^{23}$ Na spectra were referenced to 1.0 M aqueous NaCl<sub>(aq)</sub> at 0 ppm.

### 2.2.4 Fourier-transform infrared spectroscopy (FT-IR)

The chemical bonding environments present in the geopolymer waste forms was investigated using Nicolet iS10 FT-IR (Thermofisher Scientific, USA) with attenuated total

reflection (ATR). FT-IR spectra were acquired with wavenumbers between 650 and 4000 cm<sup>-1</sup>.

#### 2.2.5 Microstructure

The fresh geopolymer fracture surfaces were coated with Pt for 20 s at 20 mA and then analyzed via high resolution field-emission scanning electron microscopy (FE-SEM) for secondary imaging and energy dispersive X-ray spectroscopy (EDS) for elemental mapping using Jeol JSM-7800F with an Oxford insturments Ultim X-ray microanalysis detector.

### 2.2.6 Thermal analysis

Thermogravimetric analysis was performed using a DSC 8500 TG-DSC machine (PerkinElmer, USA) to investigate the thermal properties of geopolymer waste forms at a heating rate of 10 °C/min in an argon atmosphere from 20 to 700 °C.

#### 2.2.7 Raman spectroscopy

Raman spectra were acquired to investigate the structural changes in the simulated BW at room temperature using a Raman Spectrometer (LabRaman Aramis, Horiba Jobin-Yvon, France). The samples were stimulated with a 514 nm laser at 5 mW power using a  $50\times$  objective that focused on a 1  $\mu$ m spot. The spectral data were recorded within the 200–1200 cm<sup>-1</sup> range.

### 2.2.8 *In-situ* high-temperature XRD (HT-XRD)

*In-situ* HT-XRD analysis was conducted using an *in-situ* XRD (Empyrean, Malvern Panalytical, Netherlands) to confirm the formation of C-(A)-S-H gel and structural changes of geopolymer waste form with Ca(OH)<sub>2</sub>. Geopolymers and C-(A)-S-H gels have poor crystallinity (amorphous or semi-crystalline), making it challenging to differentiate them using

conventional XRD analysis. The use of *in-situ* HT-XRD to induce high-temperature phase transitions in geopolymers and C-(A)-S-H gels can indirectly infer their presence. Cu K radiation was used at a step size of 0.013. The operating voltage and current were 40 kV and 30 mA, respectively. The geopolymer sample was heated from room temperature (25 °C) to 700 °C at a heating rate of 10°/min. The HT-XRD patterns were collected from 10 to 60° 20 every 100 °C.

### 2.3 Leaching test

The geopolymers were subjected to 100 d long-term leaching tests in duplicate following the ANSI/ANS 16.1 procedure [29]. Monolith samples were submerged in  $629 \pm 10$  mL DIW, with the volume to surface ratio set at  $10.0 \pm 0.1$ . The leachate was refreshed at intervals of 2 h, 7 h, 1 d, 2 d, 3 d, 4 d, 5 d, 19 d, 47 d, and 100 d. The ion concentrations (B, Ca, Si, and Al) in the collected leachate was measured using an inductively coupled plasma optical emission spectrometer (ICP-OES, Optima 7300 DV, USA). The cumulative fraction leached (CFL) was dertermined based on the average ion concentration as follows:

$$CFL = \frac{\sum a_n}{A_0}, \qquad Eq. (1)$$

where  $a_n$  is the mass of releasd ions during the leaching interval n (g) and  $A_0$  is the total mass of ion in the geopolymers (g) [29]. The effective diffusivity (D<sub>e</sub>; cm<sup>2</sup>/s) was determined using Eq. (2),

$$D_e = \pi \left[ \frac{a_n / A_0}{(\Delta t)_n} \right]^2 \left( \frac{v}{s} \right)^2 T,$$
 Eq. (2)

where  $(\Delta t)_n$  is leaching interval (sec); V is the volume of geopolymer (cm<sup>3</sup>); S is sample surface area (cm<sup>2</sup>); T is the average duration of the leaching interval (sec) [29].

The leaching rate was calculated by following Eq. (3).

Leaching rate = 
$$\left(\frac{\sum a_n}{A_0}\right) \frac{v}{s} = \frac{1}{t}$$
, Eq. (3)

The D<sub>e</sub> value can be determined using Eq. (4) if the CFL exceeds 20% [29],

222 
$$D_e = \frac{Gd^2}{t}$$
, Eq. (4)

- where G is dimensionless time factor; d is the diameter of sample (cm); t is the leaching
- time since the beginning of the first leaching interval (sec) [29].
- The leachability index (Li) was determined using Eq. (5),

226 
$$\operatorname{Li} = \frac{1}{n} \sum_{i=1}^{n} \left[ \log \left( \frac{\beta}{D_e} \right) \right]_{i},$$
 Eq. (5)

- where  $\beta$  is a constant defined as 1.0 cm<sup>2</sup>/s.
- The leaching mechanism was be determined using Eq. (6),

$$Log B_t t = \frac{1}{2} log(t) + log \left[ U_{max} \rho \sqrt{\frac{D_e}{\pi}} \right],$$
 Eq. (6)

- where  $B_t$  is release in period t (mg/m);  $U_{max}$  is maximum leachable quantity (mg/kg);  $\rho$  is
- 231 the bulk density of sample (kg/m).

#### 3. Results and discussion

232

233

234

235

236

### 3.1 Effect of Ca(OH)2 on the structural characteristics of geopolymer waste form

In our previous study, the incorporation of 30 wt% BW into geopolymer waste form revealed the coexistence of diverse borate crystalline phases within the geopolymer matrix (Fig.

1) [25]. The BW in metakaolin-based geopolymer waste form is immobilized through both chemical and physical mechanisms [25]. In an alkaline environment, B tends to prefer tetrahedral coordination; thus, B dissolved by alkaline activators generally exists in a tetrahedral unit (BO<sub>4</sub>). These tetrahedral borates react with silicates, initially forming B-O-Si networks and subsequently transforming into a B<sup>III</sup>-O-Al-O-Si network [24, 25]. Conversely, physically immobilized BW persists in various borate crystalline phases within the geopolymer waste form [25]. When Ca(OH)<sub>2</sub> (s) was added to the geopolymer, the intensity of the diffraction patterns corresponding to borax ( $2\theta = 13-23$ , 35, 37–39, 43–44, and 54°), a major component of BW, gradually diminished with increasing calcium content (Fig. 1). In geopolymer with a high Ca/Al ratio (>0.75), the distinctive diffraction pattern of borax became imperceptible, and a poorly ordered semi-crystalline phase was identified at approximately 29° 2θ-region (Fig. 1). The geopolymer waste form which was fabricated in this study had complex chemistry; CaO-SiO<sub>2</sub>-Al<sub>2</sub>O<sub>3</sub>-B<sub>2</sub>O<sub>3</sub>-H<sub>2</sub>O system. Considering the abundance of aluminum in geopolymer waste form, particularly when metakaolin is used as a raw material, as was the case in this study, the observed diffraction pattern was attributed to the presence of C-(A)-S-H gel. Aluminum partially substitutes silicate in the C-S-H gel and leads to the formation of an aluminum-containing tobermorite structure which exhibits short atomic ordering similar to an amorphous or low-crystallinity structure [30]. The C-(A)-S-H gel exhibits a somewhat broad diffraction pattern which resembles a semi-crystalline or poorly ordered phase at locations akin to those observed in C-S-H gel [31]. Furthermore, a new crystalline phase such as calcium sodium pentaborate was confirmed in the geopolymer with the highest Ca/Al ratio of 1.0 alongside the C-(A)-S-H gel. The addition of Ca(OH)<sub>2</sub>(s) to the geopolymer results in pH increase due to Ca(OH)<sub>2</sub> dissolution [26]. Thus, it was assumed that physically immobilized BW decomposed due to an increase in pH at a high Ca/Al ratio and then reacted with free

237

238

239

240

241

242

243

244

245

246

247

248

249

250

251

252

253

254

255

256

257

258

259

calcium ions to produce a crystalline calcium sodium borate phase. When Ca(OH)<sub>2</sub> is incorporated into a metakaolin-based geopolymer, the solubility of Ca(OH)<sub>2</sub> is contingent upon the concentration of silicate. On the other hand, when Ca(OH)<sub>2</sub> is added to geopolymer formulations with 5M or 10M NaOH alkaline activators, the common ion effect results in Ca(OH)<sub>2</sub> remaining as a relatively inert phase and prefers to precipitate as a crystalline phase (e.g., portlandite) without complete dissolution [26]. If Ca(OH)<sub>2</sub> is added to geopolymers prepared with alkaline activators of the same concentration of sodium silicate, all the Ca(OH)<sub>2</sub> (s) dissolves [26].

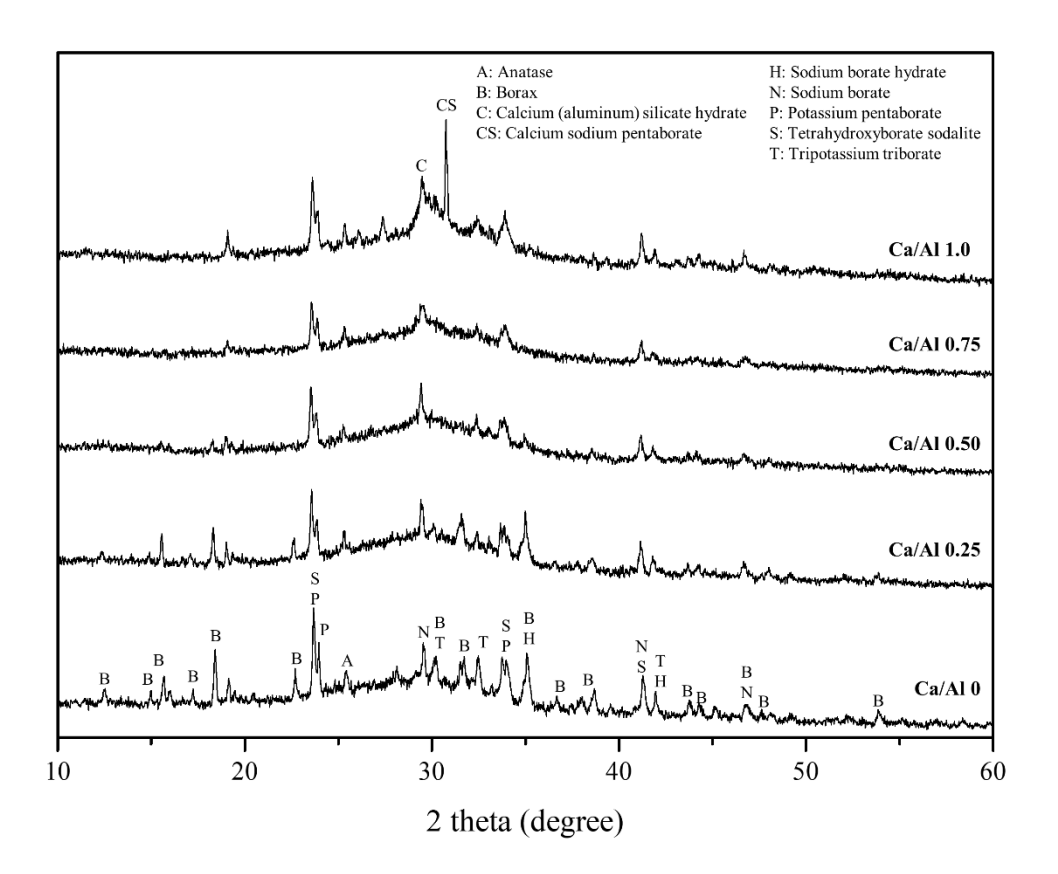


Figure 1. XRD results of geopolymer waste forms with varying Ca/Al ratios.

The results from the Raman analysis were in agreement with the XRD results. In geopolymers with relatively low Ca/Al ratios (0.25 and 0.5), clear borax peaks were observed.

However, in geopolymers with Ca/Al ratios of 0.75 and 1.0, these peaks were not detected (Fig. 2). In pure geopolymers, the broadening of three aluminosilicate bands typically occurs at 395, 509, and 635 cm<sup>-1</sup> which indicate the presence of aluminosilicate ring structures with 8membered, double 6-membered, and 4-membered rings, respectively [32]. The primary Raman peak of C-S-H or C-(A)-S-H gel is commonly reported at 671 cm<sup>-1</sup>, irrespective of the Ca/Si ratio, which corresponds to Si-O-Si symmetric bending (Q2 unit) [33]. In this study, this peak was not observed even in geopolymers with the highest calcium content (Fig. 2). This speculation results from the relatively poor crystallinity of the C-S-H or C-(A)-S-H gel formed in geopolymers, as indicated by the XRD results (Fig. 1). Additionally, a quantitative correlation with the amounts of the two generated phases (C-S-H and C-(A)-S-H) may exist. In geopolymers with a Ca/Al ratio of 1.0, the added amount of Ca(OH)<sub>2</sub> was 8.5 wt%. Even if all calcium ions are utilized in the formation of C-(A)-S-H gel, the theoretically maximum amount that can be produced is not high, as it is proportional to the added amount of Ca(OH)<sub>2</sub>. Moreover, because calcium can engage in chemical reactions such as charge balancing [34] and bonding with borates in the geopolymer system [24], it is expected to be lower than the theoretical upper limit of C-(A)-S-H gel attainable in this system. These factors are believed to contribute to the absence of peaks from the two phases in the Raman results.

273

274

275

276

277

278

279

280

281

282

283

284

285

286

287

288

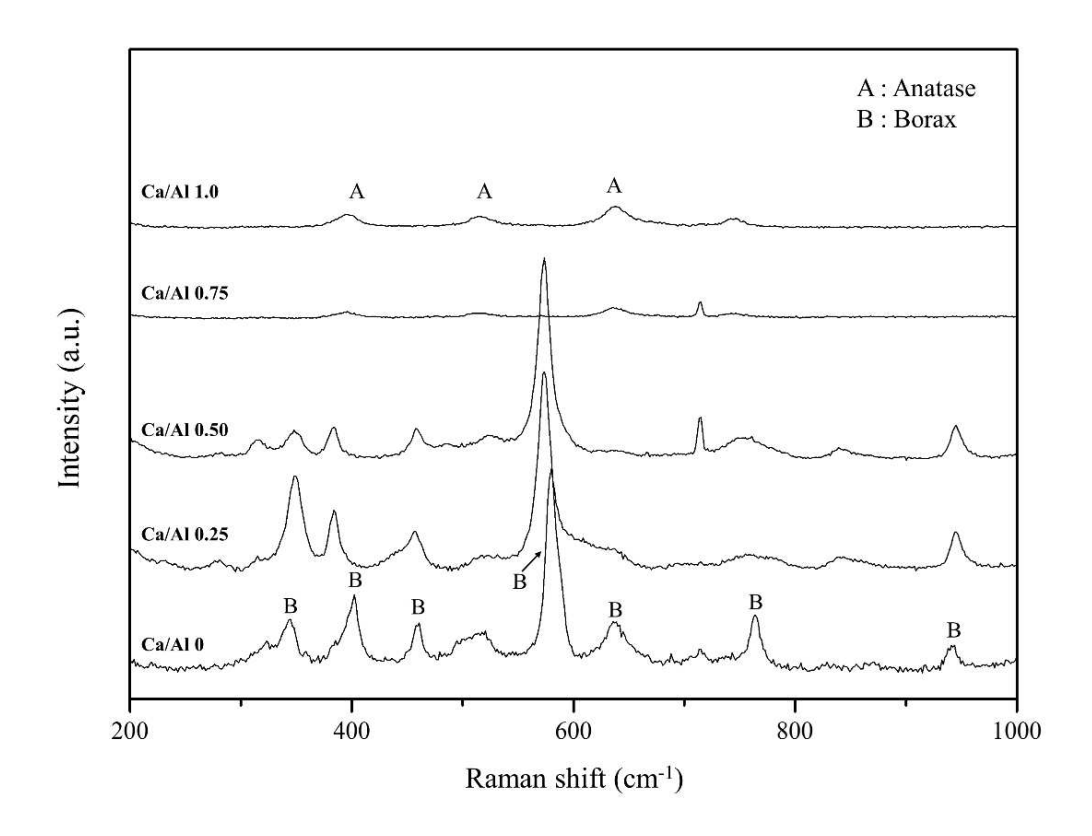


Figure 2. Raman results of geopolymer waste forms as function of Ca/Al ratios

The solid-state MAS NMR analysis results indicated a structural transformation of B and the main elements (Si and Al) of the geopolymer waste form induced by calcium (Fig. 3). The <sup>11</sup>B MAS NMR spectra clearly revealed the presence of B<sup>III</sup> in the ring structure, B<sup>III</sup> in the non-ring structure, and B<sup>IV</sup> in the geopolymer without Ca [35]. The speciation of B varies with pH, and it predominantly exists as B<sup>IV</sup> in alkaline environments, as mentioned above. Therefore, the presence of the B<sup>III</sup> peaks is attributed to physically immobilized BW in the geopolymer [25]. As the Ca/Al ratio increases, the intensity of B<sup>III</sup> in the ring and non-ring structures decreases, accompanied by a gradual broadening of the peaks (Fig. 3a). This indicates the decomposition of some physically immobilized BW after Ca(OH)<sub>2</sub> addition. In geopolymers with a high Ca/Al ratio, several crystalline phases present in the BW disappeared, and the

diffraction patterns of calcium sodium borate were detected. These results imply that a corresponding increase in B<sup>IV</sup> occurs as the quantity of B<sup>III</sup> decreases. Meanwhile, the resonance of B<sup>IV</sup> remained nearly consistent at a similar position (1 ppm), regardless of the Ca/Al ratios (Fig. 3a). The increase in B<sup>IV</sup> may indicate a rise in the quantity of B capable of reacting with Si, as it forms chemical bonds by partially substituting Si, which resembles Al. It could potentially influence the compressive strength of the geopolymer waste forms. The effect of Ca(OH)<sub>2</sub> on the compressive strength will be discussed later.

303

304

305

306

307

308

309

310

311

312

313

314

315

316

317

318

319

320

321

322

323

324

325

In the <sup>27</sup>Al MAS NMR analysis, a distinct Al<sup>IV</sup> resonance was clearly observed at 60 ppm (Fig. 3b). The Al<sup>IV</sup>, Al<sup>V</sup>, and Al<sup>VI</sup> present in metakaolin transforms into aluminosilicate gel with Al<sup>IV</sup> due to alkaline activators and form an amorphous aluminosilicate structure by binding with Si tetrahedra. The linewidth of Al<sup>VI</sup> resonance gradually increased, and chemical shielding was observed as the resonance center shifted toward lower chemical shifts with increasing Ca(OH)<sub>2</sub> content (Fig. 3b; inset). This is attributed to Ca altering the electronic cloud around Al atoms. In high Ca content gel systems (Ca/(Si+Al) = 0.67 and 1.00), Al<sup>IV</sup> resonance appears broadly in the range of 40-80 ppm [30]. These systems show the presence of Al in bridging tetrahedra, cross-linking tetrahedra, and paired tetrahedra within the C-(A)-S-H gel [30]. Considering the resonance occurring at the same position for Si and highly polymerized Al as the main unit in geopolymers, distinguishing between Al in C-(A)-S-H gel and Al within the geopolymer structure based on the results of <sup>27</sup>Al MAS NMR in this study may prove challenging. In addition, precise quantitative analysis of high-coordinated Al, such as Al<sup>V</sup> and Al<sup>VI</sup>, is challenging due to the peak broadening effect caused by the quadrupolar interaction of Al. Nevertheless, when compared to geopolymers without Ca, the qualitative observation indicates a reduction in the intensity of resonances for AlV and AlVI in geopolymers with a

Ca/Al ratio of 0.25, 0.5, and 0.75 (Fig. 3b). A previous study reported that the addition of Ca(OH)<sub>2</sub> to geopolymers reduces the formation of aluminosilicate gel on the surface of unreacted metakaolin particles [36]. This reduction is attributed to the reaction of Ca, which consumes Si in processes such as the formation of C-(A)-S-H gel. This results in the dissolution of more metakaolin, leading to a decrease in Al<sup>V</sup> and Al<sup>VI</sup> and an increase in Al<sup>IV</sup> as well [36]. Interestingly, the qualitative resonance of Al<sup>V</sup> and Al<sup>VI</sup> in the geopolymer with the highest Ca/Al ratio appeared slightly higher than that in the geopolymer without Ca(OH)<sub>2</sub> (Fig. 3b). The addition of Ca(OH)<sub>2</sub> to geopolymers significantly accelerated the setting of geopolymers and the setting time was reduced in proportion to the Ca content [36]. Therefore, in the geopolymers with the highest Ca content, the resonance intensity of Al<sup>V</sup> and Al<sup>VI</sup> appeared somewhat higher than in geopolymers without Ca addition because of the fast setting that occurs before sufficient dissolution of metakaolin.

The marked changes in the <sup>29</sup>Si MAS NMR spectra were confirmed based on the Ca/Al ratios (Figure 3c). As the Ca/Al ratio increased, the <sup>29</sup>Si resonance exhibited a higher chemical shift which indicates the occurrence of deshielding. This suggests that the environment around the Si tetrahedra was altered by the presence of Ca, similar to the <sup>27</sup>Al MAS NMR results. Geopolymers with Ca/Al ratios of 0.25 and 0.5 exhibited resonances similar to that of pure geopolymer. In geopolymer waste forms containing 30wt% BW, Q4(B) units by chemical bonding between B and Si (B-O-Si network) and Si Q sites of the geopolymer (Q4(4Al), Q4(3Al), Q4(2Al), Q4(1Al), and Q4(0Al)) were present [25]. These units were positioned at –105, –85, –89, –92, –98, and –109 ppm, respectively. In contrast, in geopolymers with high Ca/Al ratios (0.75 and 1.0), the <sup>29</sup>Si resonances became overall sharper, and the linewidth significantly reduced. The region of Q4(mAl) (m = 0, 1, 2, 3, and 4) sites which are Si units in

the geopolymer decreased and the resonance shifted from approximately -91 ppm to -83 ppm. This location is similar to the Si NMR resonances of C-(A)-S-H gel. When Ca was added to alkali-aluminosilicate gel, it results in the formation of relatively less polymerized twodimensional Qn sites such as Q1, Q2, and Q3, compared to the more polymerized Q4 sites. In the CaO-Na<sub>2</sub>O-SiO<sub>2</sub>-Al<sub>2</sub>O<sub>3</sub>-H<sub>2</sub>O system, Q0, Q1(I), Q1(II), Q2, Q2(1Al), Q3(1Al) units are observed in the range of -72 to -87 ppm with the Q2 unit showing the dominant intensity at approximately -82 ppm [34]. For further understanding of C-(A)-S-H gel formation in this study, <sup>29</sup>Si MAS NMR spectra were deconvoluted, and the results confirmed the peaks for low On sites in geopolymers with high Ca/Al ratios (0.75 and 1.0) (Fig. 4). This suggests that C-(A)-S-H gel was formed in geopolymers with high Ca/Al ratios. At low Ca/Al ratios (0.25 and 0.50), the spectrum was very similar to that of geopolymer without Ca(OH)2, making it challenging to precisely identify the formation of C-(A)-S-H gel through <sup>29</sup>Si MAS NMR (Fig. 3c). Nevertheless, the shoulder at -105 ppm was significantly reduced by Ca(OH)<sub>2</sub> addition (Fig. 3c). This indicates that Ca also influences the B-O-Si network. The addition of Ca increases the elements available to react with Si from two (B and Al) to three (B, Al, and Ca). Accordingly, the quantity of Si available for bonding with B in the Ca-added geopolymer system will decrease. Therefore, the decrease in the intensity of the Q4(B) resonance is attributed to the consumption of Si by Ca, leading to a reduction in the bonding between B and Si.

349

350

351

352

353

354

355

356

357

358

359

360

361

362

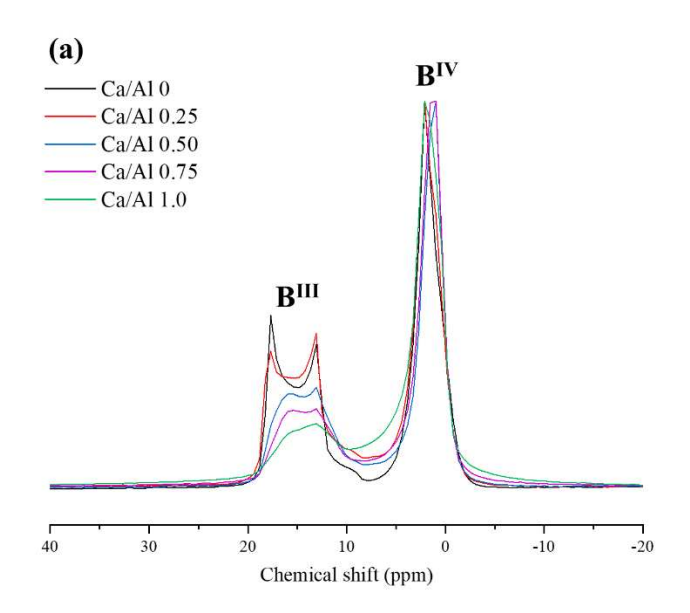
363

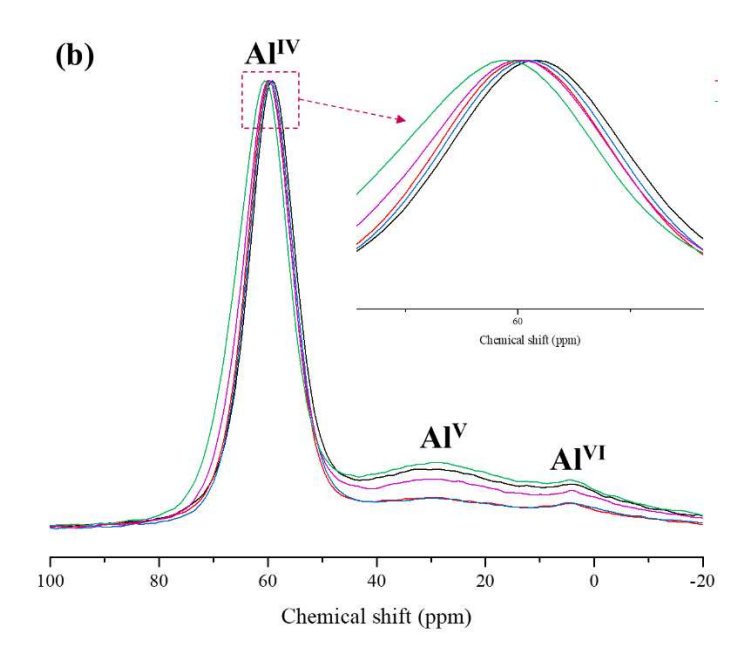
364

365

366

367





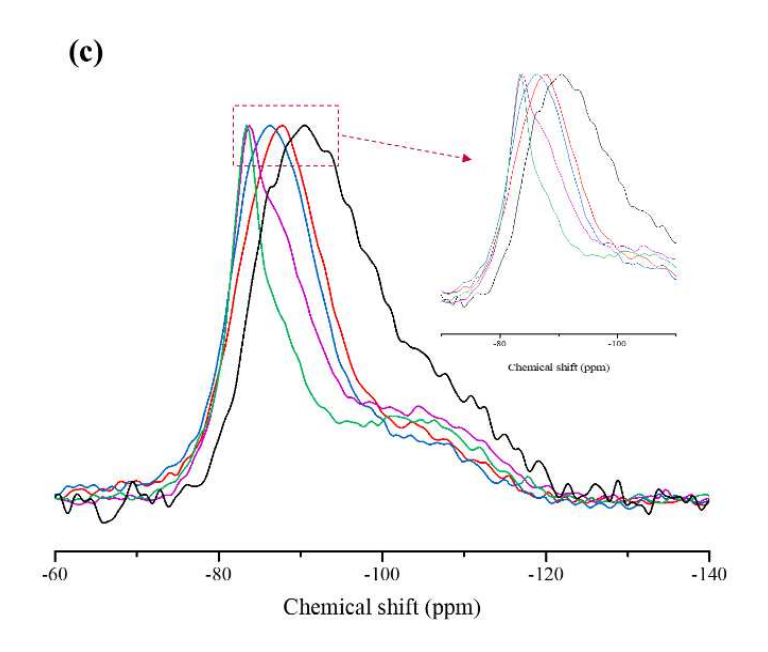


Figure 3. Solid-state MAS NMR results of <sup>11</sup>B (a), <sup>27</sup>Al (b), and <sup>29</sup>Si (c) in geopolymer waste

373 form as function of Ca/Al ratios

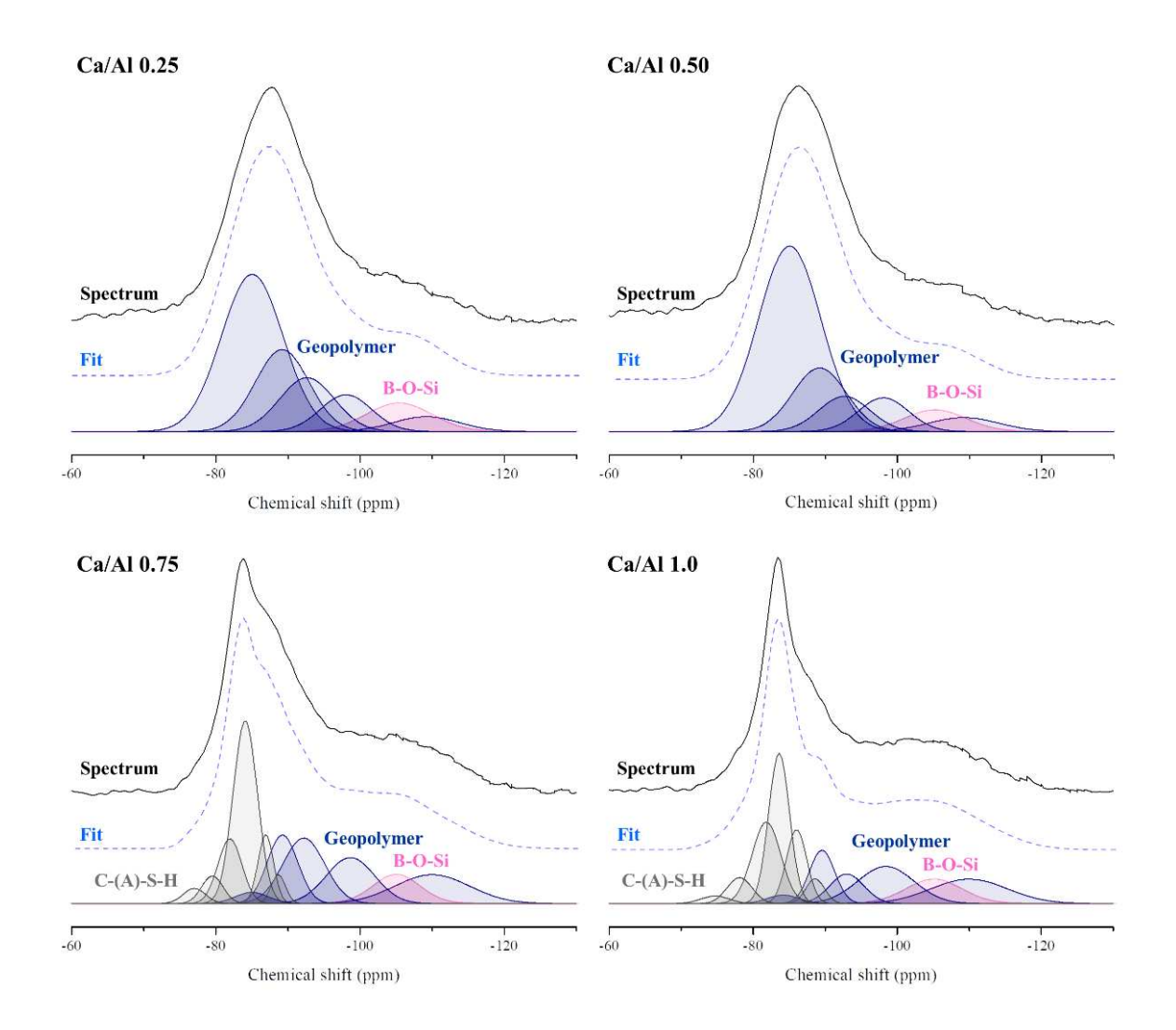


Figure 4. Deconvolution of <sup>29</sup>Si MAS NMR spectra of geopolymer waste forms

The FT-IR analysis results provide additional insights into the formation of C-(A)-S-H gel (Fig. 5). All geopolymer waste forms exhibit an intense sharp absorption band at 900–1200 cm<sup>-1</sup> which is indicative of Si-O-T (T = Si or Al). Fully separating the two phases in the FTIR results is difficult because both the main structure of the geopolymer (aluminosilicate) and the chain structure of C-(A)-S-H gel have broad peaks at similar positions [37]. However, this band gradually shifts to lower wavenumbers and sharpens as the added Ca(OH)<sub>2</sub> increases. This shift suggests higher polymerization in geopolymers and structural ordering in C-(A)-S-

H gel [37]. Therefore, the addition of Ca(OH)<sub>2</sub> contributes to the reactions in geopolymers and the formation of C-(A)-S-H gel, as indicated by previous results [31, 36]. The broad band at 1370 cm<sup>-1</sup> is also attributed to B-O bonding, and the sharpening of this band with Ca(OH)<sub>2</sub> addition results from structural changes in BW (e.g., the formation of calcium borate). The band at 1648 cm<sup>-1</sup> was related to the absorbed atmospheric water [14].

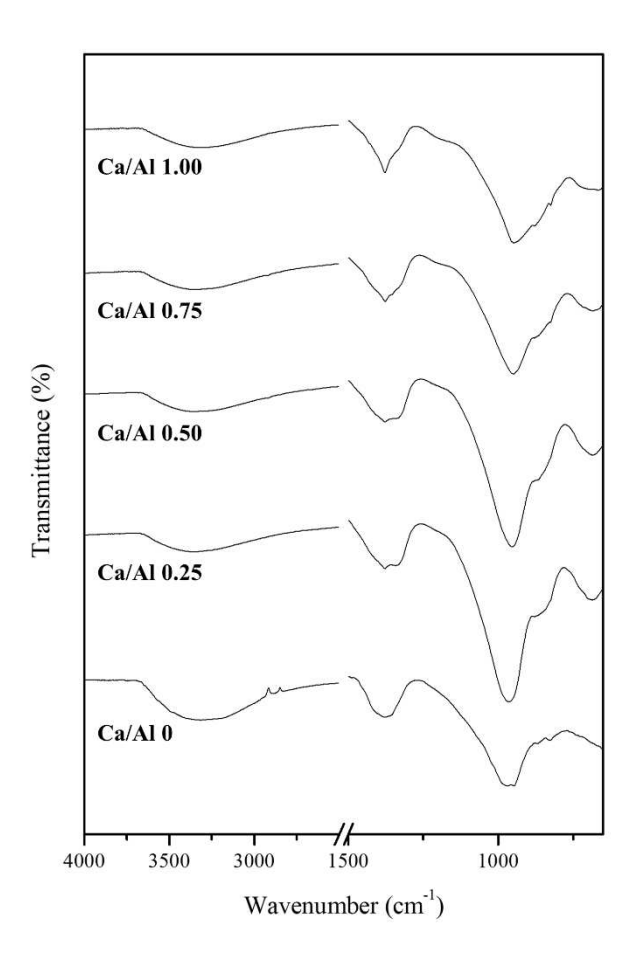


Figure 5. FT-IR results of geopolymer waste forms with varying Cal/Al ratios

# 3.2 Enhanced compressive strength of geopolymer waste form by Ca(OH)<sub>2</sub>

The compressive strength of geopolymer waste forms after 7 days of curing was not proportional to the Ca/Al ratio; however, geopolymers containing Ca(OH)<sub>2</sub> exhibited higher

compressive strength overall compared to those without Ca(OH)<sub>2</sub> (Fig. 6). Compressive strength increased 2-3 times depending on the the Ca/Al ratios, peaking at 14 MPa for the geopolymer with a Ca/Al ratio of 0.25 (Fig. 6). Subsequently, it gradually decreased as the Ca/Al ratio increased, and the geopolymer with the highest Ca/Al ratio exhibited a strength of 10 MPa (Fig. 6). The addition of Ca(OH)<sub>2</sub> to geopolymers results in variations in the physical properties such as setting and compressive strength, depending on the Ca source used. The incorporation of Ca additives such as CaCO<sub>3</sub> (calcite), changes the physical properties of geopolymers according to the content. The addition of a small amount of calcite (<12%) does not cause significant changes in the compressive strength, setting mechanism, and activation energy of geopolymers [38]. This is attributed to the poor solubility of calcite in basic solutions [38]. Using an optimal quantity of calcite (20%) enhanced the 7-day compressive strength of metakaolin-based geopolymer from 36.2 MPa to 44.4 MPa; conversely, exceeding 40% led to the low compressive strength (to 23.7 MPa) [38]. The compressive strength decreased in proportion to the calcite content which is attributed to changes in the degree of geopolymer gel formation, shrinkage, and microstructure connectivity [39]. The effects of CaO or Ca(OH)<sub>2</sub> addition are known to be similar to those of CaCO<sub>3</sub>; however, introducing a lesser quantity than CaCO<sub>3</sub> is beneficial for enhancing the physical characteristics of the geopolymer [28, 40]. In particular, Ca(OH)<sub>2</sub> accelerates the setting, and the appropriate amount of addition increases the compressive strength. Adding 2% Ca(OH)<sub>2</sub> to the geopolymer using a sodium silicate solution (Na<sub>2</sub>O:Al<sub>2</sub>O<sub>2</sub>:4SiO<sub>2</sub>:11H<sub>2</sub>O) results in a slight improvement in the 7-day compressive strength from 68 MPa to 76 MPa [28].

395

396

397

398

399

400

401

402

403

404

405

406

407

408

409

410

411

412

413

414

415

416

417

The fast setting and compressive strength variation induced by the addition of Ca(OH)<sub>2</sub> are primarily attributed to the fast dissolution of metakaolin and C-(A)-S-H gel formation. The

Al species in metakaolin are converted to aluminosilicate (Al<sup>IV</sup>) after exposure to alkaline activators. This then participates in a polycondensation reaction (geogpolymerization reaction) and binds with Si tetrahedra, which results in the formation of a geopolymer gel structure. The addition of Ca(OH)2 influences the formation of Al<sup>IV</sup> in the geopolymer. During the initial stages (<5 h) of the geopolymerization reaction facilitated by Ca(OH)<sub>2</sub>, the quantity of Al<sup>IV</sup> significantly increases from approximately 55% to 90% [36]. The quantity AlV and AlVI decreases with an increase in Al<sup>IV</sup> [36]. The dissolution of precursor material is accelerated as the Ca content increases and most of the Al(OH)<sub>3</sub>, which serves as the Al source in precursor material, is dissolved within 30 h of the geopolymerization reaction when the Ca/Si ratio reaches 2.0 [31]. The Al released from metakaolin easily reacts with Si and precipitates aluminosilicate gel on the surface of unreacted metakaolin, limiting its further dissolution (the protective layer effect) [36]. In other words, the presence of Ca decreases the Si concentration because Si reacts with Ca, leading to a reduction in the formation of gel precipitation on the metakaolin surface. The reaction between Si and Ca may be related to the formation of C-(A)-S-H gel. In alkali-aluminosilicate systems containing Ca, the C-(A)-S-H gel may easily precipitate due to the Al content in the geopolymer being considerably higher than in the OPC. Unlike in a geopolymer, where Al and Si tetrahedra may form a random three-dimensional structure, the C-(A)-S-H gel consists of Ca and Si (Al) arranged in a two-dimensional chain structure [30]. According to the X-ray pair distribution function analysis of geopolymers containing Ca, the CaO<sub>7</sub> polyhedra constituting the C-(A)-S-H gel exhibits a correlation peak at 2.4 Å. The Ca-O layers became more ordered as the Ca content increased, and the intensity of correlation peaks containing Ca such as Ca-T (T=Si or Al), Ca-Ca, and Ca-O increased [31]. This indicates that the C-(A)-S-H gel coexists with the geopolymer structure when geopolymers contain Ca.

418

419

420

421

422

423

424

425

426

427

428

429

430

431

432

433

434

435

436

437

438

439

440

In general, the addition of Ca(OH)<sub>2</sub> to geopolymers incoporating 30 wt% of BW resulted in a 2–3 fold compressive strength improvement. The results suggest that the enhancement in compressive strength can be attributed to the fast dissolution of metakaolin by Ca(OH)<sub>2</sub> and the formation of C-(A)-S-H gel. As discussed in the XRD and <sup>29</sup>Si MAS NMR results, the addition of Ca(OH)<sub>2</sub> resulted in the formation of C-(A)-S-H gel and a reduction in the bonding between B and Si (Fig 1 and 3c). In the presence of Ca, formation of C-(A)-S-H gel consumes Si, leading to a decrease in the overall available Si amount for the reactive B-O-Si network formation. The chemical bonding between B and Si is slower than Si-O-Al bonding, as it forms B<sup>III</sup>-O-Al-O-Si bonds in advance by reacting with Al [24]. The reaction rate slows further with an increase in BW content, resulting in a decrease in the compressive strength of the geopolymer waste form [25]. Therefore, the reduction of the amount of B-O-Si bonding due to the presence of Ca is thought to contribute to an increase in the compressive strength by decreasing the slower-reacting bonds (B-O-Si and B<sup>III</sup>-O-Al-O-Si) within the geopolymer matrix.

Meanwhile, the compressive strength decrease in geopolymers with high Ca/Al ratios is attributed to the reduction in the workability and flowability of the geopolymer paste due to its fast setting, leading to inadequate molding (Fig. 6). When 4% of Ca(OH)<sub>2</sub> was added to metakaolin-based geopolymer with a SiO<sub>2</sub>:Al<sub>2</sub>O<sub>3</sub>:Na<sub>2</sub>O:H<sub>2</sub>O molar ratio of 1:1:4:11, the final setting time decreased considerably (from 19 h to 2 h), and the 7-day compressive strength also decreased from 76 MPa to 56 MPa [28]. Therefore, adding Ca(OH)<sub>2</sub> is effective for enhancing the physical properties of geopolymer waste forms containing BW; however, an appropriate amount of Ca(OH)<sub>2</sub> should be considered to ensure effectiveness while avoiding fast setting.

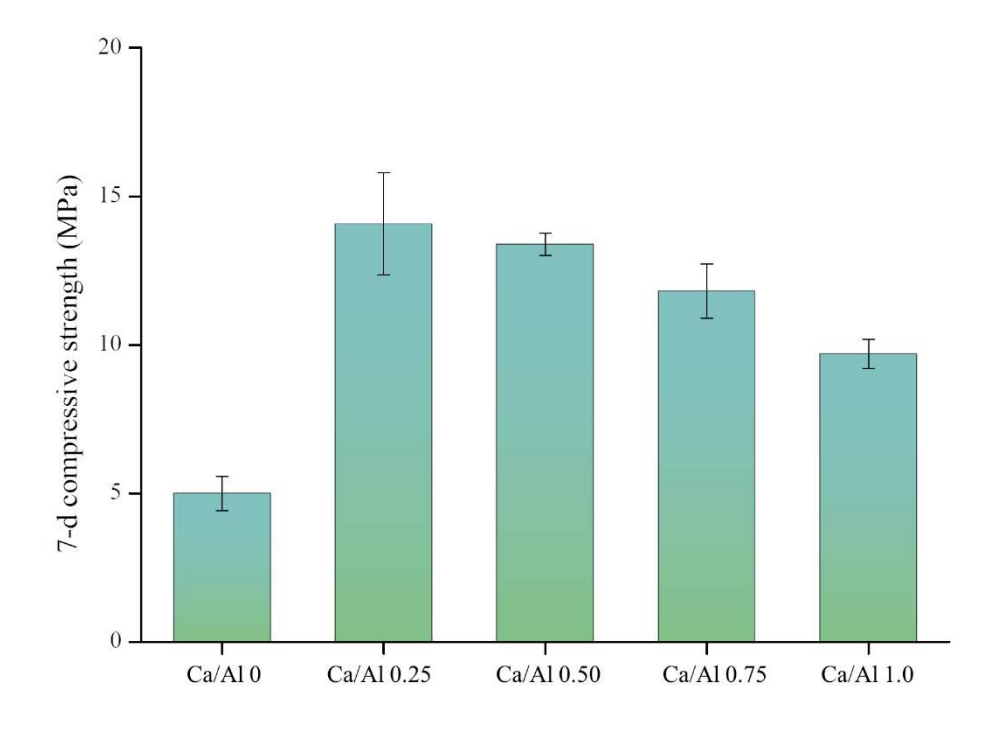


Figure 6. 7-day compressive strength results of geopolymer waste forms with varying Ca/Al ratios

# 3.3 Further insights into C-(A)-S-H gel formation and geopolymer gel structure evolution

The thermal analysis results provide indirect information about the quantity of geopolymer gel products formed (Fig. 7). The water in the geopolymer system exists as both free and structural water. Free water refers to the water remaining in the pores, which undergoes decomposition at approximately 120 °C [41, 42]. In contrast, structural water in geopolymer refers to water molecules that are bound to the amorphous aluminosilicate gel structure, and this structural water undergoes decomposition in the range of 120–700 °C [42]. If the mass loss of geopolymer with increasing temperature is greater in the range indicating structural water, this indirectly suggests that more geopolymer has been formed [41]. The addition of Ca is thought to accelerate the geopolymer reaction and lead to the formation of C-(A)-S-H with structural water. Despite our expectation that the overall mass loss would be proportional to

the Ca/Al ratios, the result revealed a non-proportional relationship of the order Ca/Al 0 < Ca/Al 1.0 < Ca/Al 0.5 < Ca/Al 0.25 < Ca/Al 0.75. This is attributed to the combined effects of Ca(OH)<sub>2</sub> addition influencing not only the formation of C-(A)-S-H but also contributing to the fast setting of geopolymer and reduced workability of the paste, among other effects. These factors collectively result in an inconsistent trend. In addition, various crystalline phases present in BW containing structural water may also contribute to the lack of a consistent mass loss result because these crystalline phases are likely influenced by the addition of Ca(OH)<sub>2</sub> (Fig. 1). Nevertheless, the ratios of mass loss for Ca/Al 0.25, Ca/Al 0.5, Ca/Al 0.75, and Ca/Al 1.0 formulation were 24.24%, 21.04%, 27.31, and 19.40%, respectively. All geopolymer waste forms containing Ca(OH)<sub>2</sub> exhibited higher mass losses than the geopolymer without Ca(OH)<sub>2</sub> (18.92%), regardless of Ca/Al ratios. This indicates that the addition of Ca(OH)<sub>2</sub> led to the generation of more gel products (here, geopolymer and C-(A)-S-H), considering the result in Session 3.1 and 3.2.

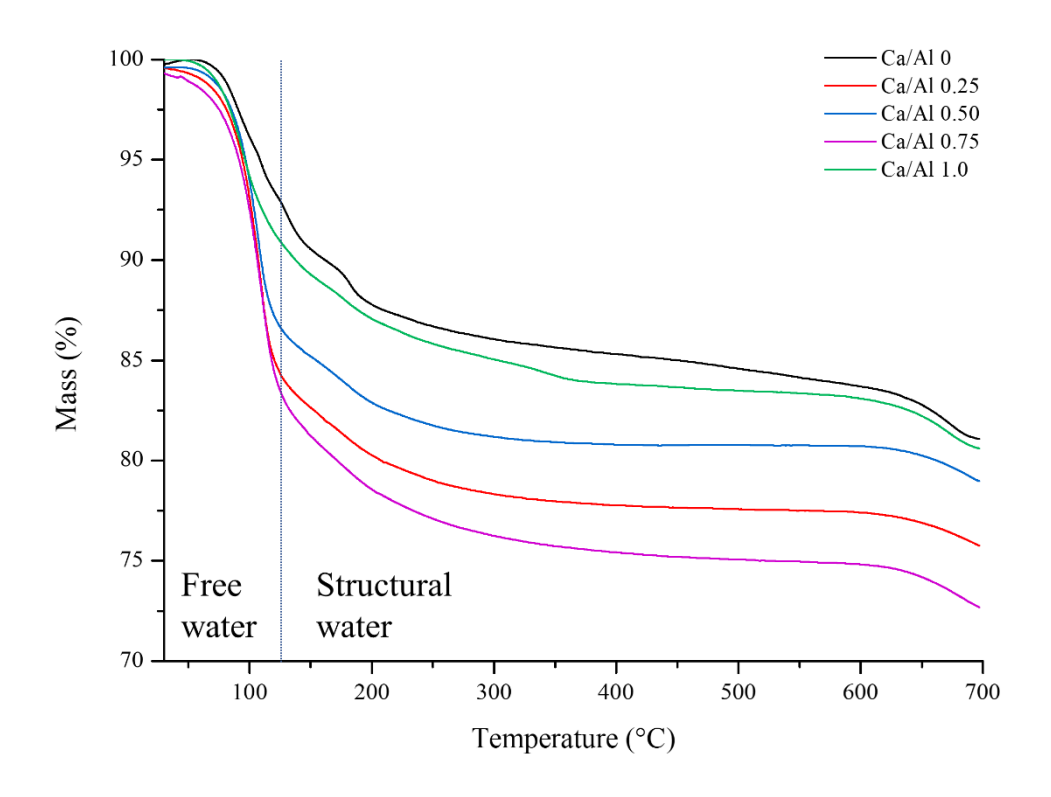


Figure 7. Mass loss (~700 °C) of geopolymer waste forms as function of Ca/Al ratios

492

493

494

495

496

497

498

499

500

501

502

503

504

505

506

507

508

509

510

511

512

513

514

*In-situ* high-temperature (700 °C) XRD analysis was performed on the geopolymer to explore the influence of Ca on the amorphous structure of the geopolymer waste form containing BW while specifically examining high-temperature phase transformations (Fig. 8). The amorphous phase of aluminosilicate in geopolymers is known to undergo a transition at approximately 700 °C, and the high-temperature crystalline phases of geopolymers vary according to the type of alkaline cation and the Si/Al ratio [43, 44]. Geopolymers activated with Na-silicate as the alkaline activator crystallizes into nepheline (or low-carnegieite) and Sirich nepheline when the Si/Al ratio is 1 or 2, respectively [26, 28, 43]. On the other hand, when K-silicate activator is used, the transformation into kalsilite (Si/Al=1) or leucite (Si/Al=2) occurs depending on the Si/Al ratio [44, 45]. In this study, the fabricated geopolymers used a K-silicate solution as the alkaline activator and with a targeted Si/Al molar ratio of 1.4; therefore, the high-temperature crystalline phase of the geopolymer is likely kalsilite. The insitu high-temperature XRD result of the geopolymer waste form without Ca(OH)<sub>2</sub> revealed diffraction patterns of kalsilite with very low crystallinity (Fig. 8). This indicates that the actual Si/Al ratio in the geopolymer was lower than the target ratio, which is likely due to the consumption of Si through the bonding of B.

Meanwhile, Ca has been reported to influence the formation of high-temperature crystalline phases in geopolymers. Kim et al. (2023) reported distinct diffraction patterns of Sirich nepheline when Ca(OH)<sub>2</sub> was added to a metakaolin-based geopolymer using a Na-silicate solution as the alkali activator [28]. This indicates that the addition of Ca accelerates the dissolution of metakaolin in the early stages of the geopolymer reaction, leading to a higher amorphous content in geopolymer which can transform into high-temperature crystalline

phases. This study yielded similar findings, where the addition of Ca(OH)<sub>2</sub> resulted in a clearer diffraction pattern of kalsilite overall (Fig. 8). The main diffraction pattern intensity of kalsilite (20 28.6°) was not proportional to the Ca/Al ratio. Geopolymers with low Ca/Al ratios (0.25 and 0.50) exhibited the most distinct diffraction pattern, whereas the intensity gradually decreased in geopolymers with a Ca/Al ratio of 0.75 and 1.0. This aligns with previous research findings in which the compressive strength increased with the Ca content and subsequently decreased at high Ca content (Fig. 6). Therefore, Ca(OH)2 addition to the geopolymer waste form promotes the formation of an amorphous structure, but excessive addition can negatively impact the geopolymer waste form because fast setting induced by excessive addition of Ca(OH)<sub>2</sub> can result in the poor workability and low compressive strength. Crystalline calcium silicate, which is related to the high-temperature phase of C-(A)-S-H gel, was observed in geopolymer with Ca/Al ratios of 0.5 and 0.75 (Fig. 8). The diffraction pattern of this phase disappeared, and gehlenite (Ca<sub>2</sub>Al<sub>2</sub>SiO<sub>7</sub>) was observed as identified in geopolymers with the highest Ca/Al ratio (Fig. 8). The exact reason for the variation in the crystalline phases formed with the Ca/Al ratio is not precisely understood; however, in-situ high-temperature XRD analysis provides clear information about the formation of C-(A)-S-H gel. In geopolymers with a Ca/Al ratio of 0.5, the presence of calcium silicate was observed in instances where the evidence of C-(A)-S-H gel formation was not shown in XRD and <sup>29</sup>Si MAS NMR analysis results. This indicates that the formation of amorphous C-(A)-S-H gel occurred even at a low Ca/Al ratio. Therefore, C-(A)-S-H formation is also speculated to have occurred in geopolymers with the lowest Ca content, but the quantity of geopolymer was so small as to be unverifiable.

515

516

517

518

519

520

521

522

523

524

525

526

527

528

529

530

531

532

533

534

535

536

537

Interestingly, K-bearing nepheline, where K partially substituted Na, was identified in

geopolymers with added Ca(OH)<sub>2</sub> (Ca.Al 0.25, 0.5, and 0.75) (Fig. 8). This suggests that Na ions released during the dissolution of BW by the alkaline activator play a charge-balancing role in the geopolymer structure, similar to K. In other words, it can be inferred that geopolymer waste form containing BW and Ca(OH)<sub>2</sub> coexists with three different phases: K-aluminosilicate, Na-aluminosilicate, and C-(A)-S-H gel. The diffraction pattern of K-bearing nepheline disappeared in the geopolymer with a Ca/Al ratio of 1.0, and it exhibited a low crystallinity, similar to the diffraction pattern of the geopolymer without Ca(OH)<sub>2</sub>. The excessive addition of Ca(OH)<sub>2</sub> leads to a complex interplay of factors, such as fast setting and the protective layer effect, as discussed in Session 3.2. Therefore, the quantity of formed geopolymers is expected to be less than that in geopolymers with an optimal amount of added Ca(OH)<sub>2</sub>.

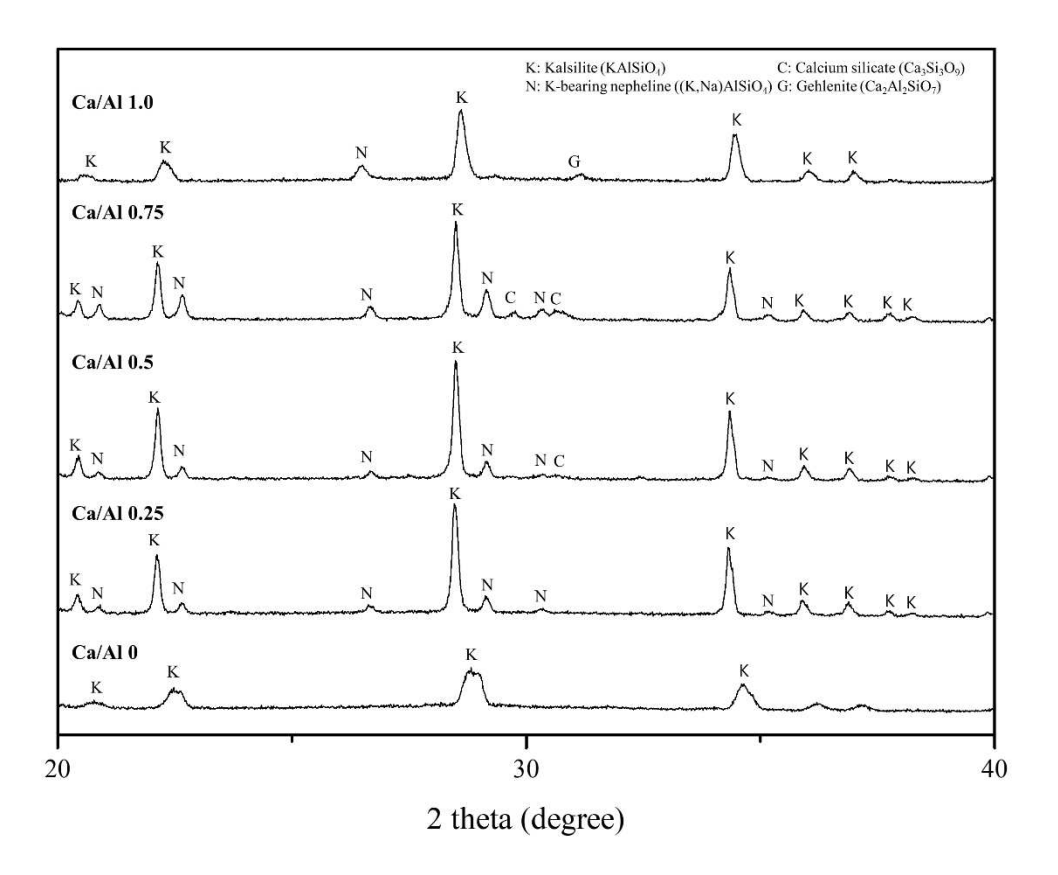


Figure 8. *In-situ* high-temperature (700 °C) XRD results of of geopolymer waste forms with

#### varying Ca/Al ratios

551

552

553

554

555

556

557

558

559

560

561

562

563

564

565

566

567

568

569

570

571

572

573

In addition, <sup>23</sup>Na MAS NMR was performed to determine whether Na released from BW participates in the geopolymerization reaction (Fig. 9). The resonances in the <sup>23</sup>Na MAS NMR of the geopolymer with Na-silicate as the alkaline activator vary somewhat depending on the Si content [46, 47]. Where the Si/Al ratio is low (<1.6), narrow, sharp, and broad peaks were observed at 0 ppm and -4 ppm, respectively. These are attributed to aqueous Na which provides a charge-balancing function for Al(OH)<sub>4</sub> in the pore solution of the geopolymer and Na associated with Al plays a charge-balancing role within the binder framework [46, 47]. If the Si/Al ratio is 1.6 or higher, only a single broad peak at -4 ppm is observed [46, 47]. Quadrupolar nuclei, such as <sup>11</sup>B, <sup>23</sup>Na, and <sup>27</sup>Al, exhibit broadened resonances due to the quadrupolar coupling effect. In this study, a single asymmetric broad peak at -2 ppm observed in all geopolymer waste forms represents that Na ion compensates for the negative charge of the geopolymer structure (Fig. 9). The chemical shift of the resonance slightly toward a positive value occurred as the Ca/Al ratio increased (from -1.5 to -0.9 ppm), and the shape of the peak gradually became more symmetric. Therefore, it can be inferred that some of the Na ions released from BW participate in geopolymer reactions, thereby supplementing the charge of the aluminosilicate framework even in the absence of Ca(OH)<sub>2</sub>. The main resonance gradually becomes more symmetric with the increase in the Ca/Al ratio (Fig. 9). Considering the finding from *in-situ* high-temperature XRD, which confirmed the presence of K-bearing nepheline, an increased Ca/Al ratio can be considered to lead to the formation of more Na-aluminosilicate geopolymer structures. Two peaks with small shoulders were identified at approximately 3 ppm and 13 ppm, respectively (Fig. 9). Although these are believed to be related to BW, precise identification posed a challenge, because the diverse sodium borate crystal phases present in

the BW can either transform into different crystalline phases or remain physically immobilized during geopolymerization reactions.

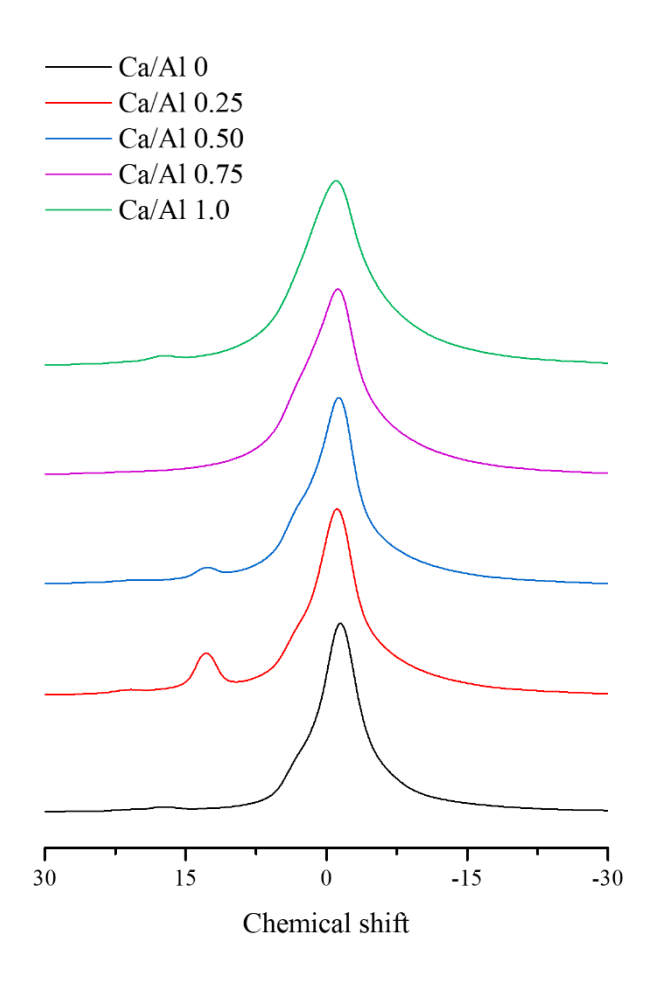


Figure 9. Solid-state MAS NMR results of <sup>23</sup>Na in geopolymer waste form with varying

### 3.4 Microstructure and surface characteristics

Ca/Al ratios

The microstructure of metakaolin-based geopolymers varies with the Si/Al ratio. Geopolymers with Si/Al ratios below 1.4 are known to exhibit a somewhat rough microstructure, whereas those with higher ratios are recognized as their well-connected and

compact surfaces [48]. The microstructure of the geopolymer without Ca(OH)<sub>2</sub> was generally somewhat rough with small particles agglomeration (Fig. 10), which is consistent with previous research results [48]. In contrast, the surface of the geopolymer with Ca(OH)<sub>2</sub> exhibited an overall smooth and compact gel-like structure (Fig. 9) similar to the surface of geopolymers with a high Si/Al ratio (Si/Al > 1.6) [48]. These results suggest that the introduction of Ca not only facilitates the fast dissolution of metakaolin and the formation of C-(A)-S-H gel, as discussed earlier, but also plays a pivotal role in influencing the evolution of the microstructure. The formation of C-(A)-S-H gel is known to contribute to the evolution of a dense and compact microstructure [40, 49].

The EDS mapping analysis was also conducted for the geopolymers with a Ca/Al ratio of 0.75 and 1.0, respectively and the results revealed different chemical composition and microstructures (Fig. 10). In the geopolymer waste form with a Ca/Al ratio of 0.75, major elements, such as Si, Al, K, Na, and Ca were uniformly distributed overall. This is consistent with the *in-situ* high-temperature XRD results (Fig. 8) which show that the fabricated geopolymer waste form consists of three different phases: Na-aluminosilicate, K-aluminosilicate, and C-(A)-S-H gel. The dominance of B and Na indicates physically immobilized BW in geopolymer, as they are primary components of BW. In geopolymers with Ca/Al ratios of 0.75 and 1.0, the presence of irregularly shaped particles ranging in size from tens of micrometers was observed on the surface of the geopolymers (Fig. 10). This phenomenon was most pronounced in geopolymers with a Ca/Al ratio of 1.0, and the presence of K<sub>2</sub>CO<sub>3</sub> was confirmed through EDS point analysis. In this study, the geopolymers had a Si/Al ratio of 1.4, and the theoretically required K/Al ratio for charge balancing is 0.4. However, an inadequate alkaline concentration can impede the effective dissolution of raw materials,

which poses challenges to geopolymer formation and results in poor physical characteristics such as low compressive strength. The geopolymer waste form was fabricated with a K/Al ratio set to 1.0, providing a K-rich environment within the paste compared to the theoretically required amount. Consequently, excess K ions were retained within the geopolymer pores. Soluble alkali metal ions diffuse outward, which leads to the surface enrichment of soluble ions and the formation of crystalline precipitates as water evaporates (e.g., white precipitates; efflorescence). This process also includes the precipitation of carbonated products such as  $K_2CO_3$  [50]. Additionally, Ca can play a nondominant role in charge balancing within the aluminosilicate structure [51]. Finally, the addition of  $Ca(OH)_2$  causes to balancing the charge by providing additional alkaline cations. The presence of more K than the theoretically required amount, along with the potential charge balancing role of Ca, is suggested to involve a complex interplay of factors that lead to the distinct formation of  $K_2CO_3$  in geopolymers with high Ca/Al ratios (> 0.75).

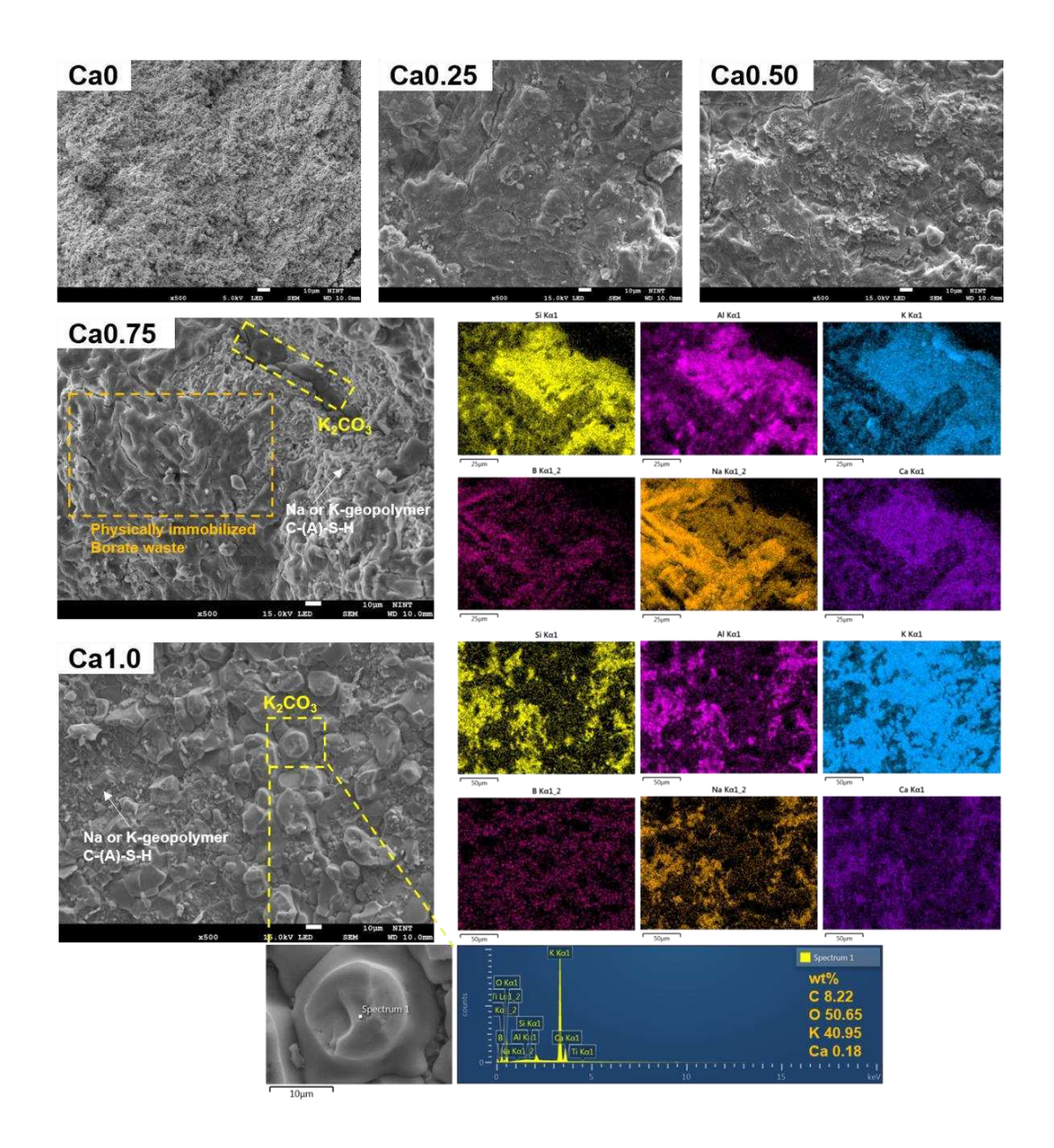


Figure 10. SEM/EDS results of geopolymer waste forms with varying Ca/Al ratios

# 3.5 Leaching characteristics and kinetics

The 100-day long-term leaching test performed on the geopolymer waste form revealed that the CFL of the primary elements of geopolymer such as Si and Al was below 0.6%, regardless of the Ca/Al ratios (Fig. 11). This shows that the addition of Ca(OH)<sub>2</sub> did not

significantly influence the leaching of either element. The CFL of Ca was somewhat higher than those of Si and Al, but it also remained low below 10% (Fig. 11). These results demonstrate that the geopolymer waste form has excellent leaching resistance, and the structure is well-maintained even after long-term leaching. The CFL of B did not change proportionally with the addition of Ca/Al ratios; however, the addition of Ca(OH)<sub>2</sub> contributed to improved leaching resistance for B (Fig. 10). The most effective Ca/Al ratio in reducing the CFL of B was 23%, with CFL decreasing from 42% to 18%, which represents more than a twofold reduction (Fig. 11). The CFL of B for Ca/Al ratios of 0.5, 0.75, and 1.0 geopolymer waste forms were 34%, 30%, and 32%, respectively, revealing a minor decrease compared to the CFL of 42% for the geopolymer waste form without Ca(OH)<sub>2</sub> (Fig. 11) [25].

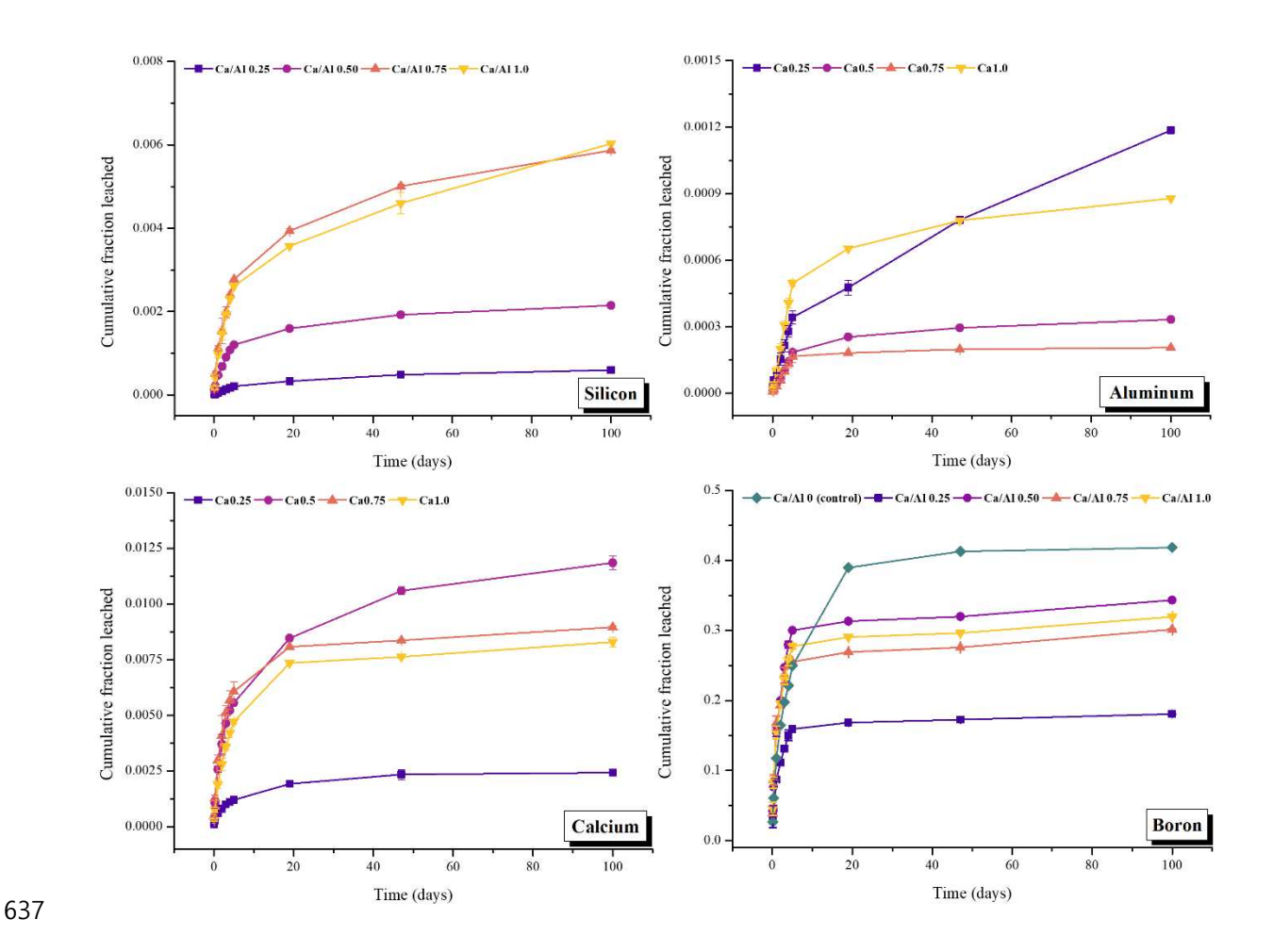


Figure 11. Cumulative fraction leached (CFL) of major elements (Ca, Al, Si, and B) in geopolymer waste forms with varying Ca/Al ratios; leaching tests were perfroemd in duplicate, and erro bar is standard deviation.

638

639

640

641

642

643

644

645

646

647

648

649

650

651

652

653

654

655

656

657

658

659

660

The slope of the linear regression was calculated using the logarithm of B<sub>t</sub> versus the logarithm of time to determine the leaching mechanism. If the slope is less than 0.35, the controlling leaching mechanism will be the surface wash-off. Slope values within the range of 0.35–0.65 indicate that leaching is controlled by a diffusion mechanism, whereas higher slope values suggest the dissolution mechanism. In this study, the overall slope exhibited values consistently lower than 0.35 and it suggests that the leaching mechanism is governed by surface wash-off (Fig. 12). Interestingly, the log(B<sub>t</sub>) values for the geopolymer with a Ca/Al ratio of 0.25 increased during the initial leaching period (~5 days) and then decreased during long-term leaching periods (19–100 days). This suggests that B in the geopolymer with a Ca/Al ratio of 0.25 follows a combination of two leaching mechanisms rather than a single leaching mechanism. The slope for the long-term leaching period was 0.21, which indicates surface wash-off. Determining the leaching mechanism based on Eq.7 was challenging due to the low R<sub>2</sub> value of 0.13 (Fig. 12). Nevertheless, the CFL of B increased very slightly during the longterm leaching intervals and reached equilibrium. The markedly low leaching of primary elements (Si and Al) and the reduced leaching rate of B suggest that the leaching mechanism of B in the geopolymer waste form with a Ca/Al ratio of 0.25 during the long-term intervals involves ion diffusion through the porous matrix (Fig 11 and 14). The reduction in silicate due to the formation of C-(A)-S-H gel is considered to contribute to the decrease in chemically immobilized BW (B-O-Si network), which leads to the observed changes in the leaching mechanism of B. The B-O-Si network maintains its structure well even after a long-term leaching test [25]. The distinct decrease in the resonance of B-O-Si in the <sup>29</sup>Si MAS NMR results (Fig. 3c) indicates a reduction in the chemical bonding between B and Si. As it decreases, the relative amount of borate that can be easily released within the geopolymer waste form is expected to increase. It results in the rapid leaching of B during the initial leaching, which indicates that B in the geopolymer follows a surface wash-off mechanism. Subsequently, leaching of B gradually reaches equilibrium, and the leaching mechanism is controlled by diffusion. The geopolymer with a Ca/Al ratio of 0.25 exhibited a compact microstructure while simultaneously exhibiting extensive geopolymer formation (highest compressive strength, low high-coordinated Al, and distinct formation in the high-temperature crystalline phase of the geopolymer) (Fig. 3b, 6, 8, and 10). These aspects likely contributed to changes in the leaching mechanisms and a reduction in the CFL of B.

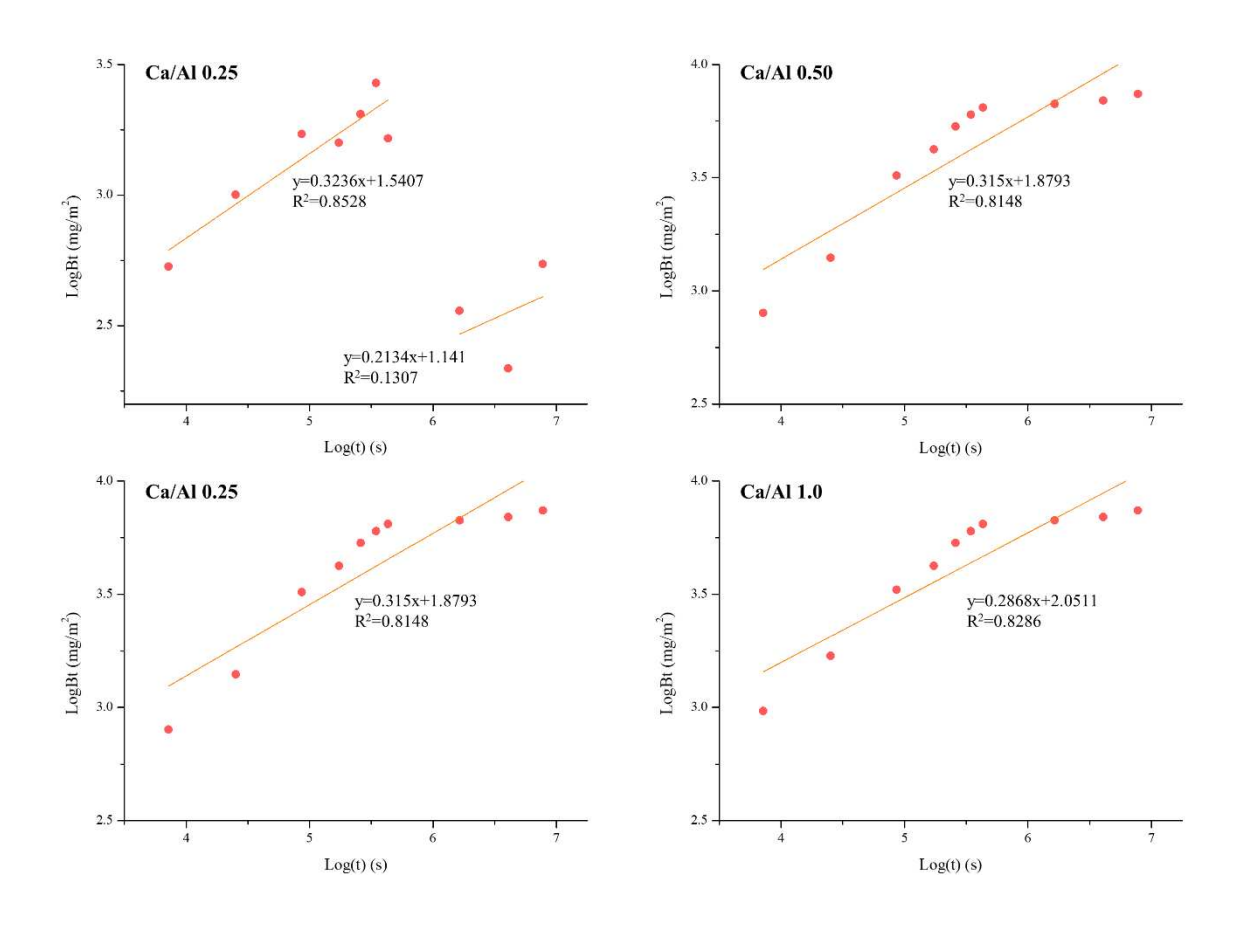


Figure 12. Slope value of linear regression of geopolymer waste forms with varying Ca/Al ratios

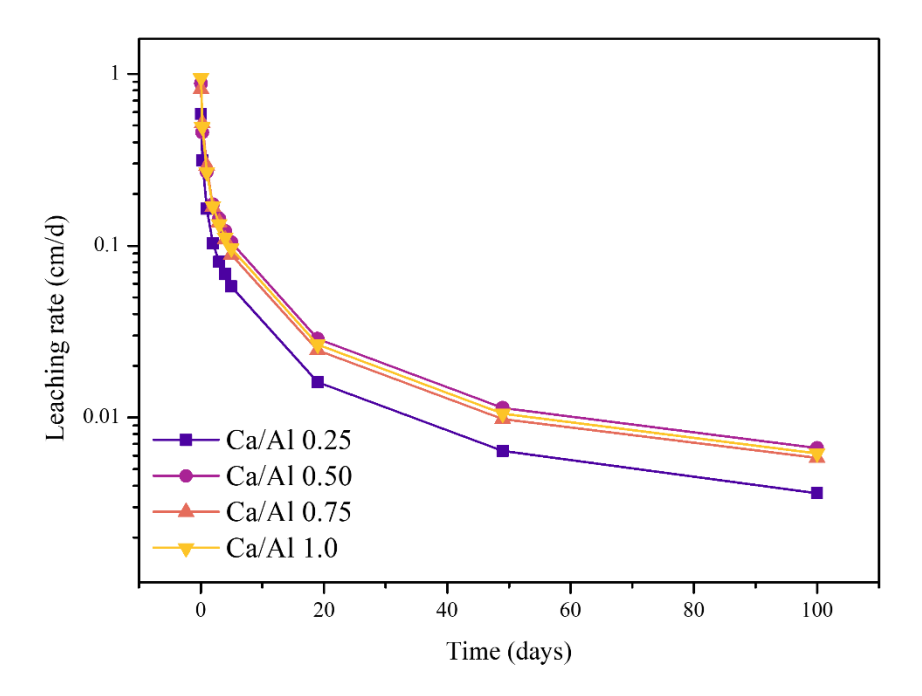


Figure 13. Leaching rate of B in geopolymer waste forms with varying Ca/Al ratios

The 100-day average Li of B was 8.7 in the geopolymer with a Ca/Al ratio of 0.25, which was approximately 1.2 times that of the previously reported value of 7.5 [25]. This is consistent with the result that the value of CFL decreased by approximately half (Fig. 11). When the Ca/Al ratio exceeded 0.25, the Li exhibited little difference from the geopolymer without Ca(OH)<sub>2</sub> and ranged from 7.4 to 7.5. South Korea has no criterion for the Li of B; however, waste forms must exceed the minimum acceptable Li of 6.0 for Cs, Sr, and Co [25]. The higher CFL and lower Li observed in geopolymers with a higher Ca(OH)<sub>2</sub> content can be attributed to the decomposition of physically immobilized BW, specifically the crystalline borate phase, which results from the excess addition of Ca(OH)<sub>2</sub>. The BW is physically immobilized and exists in various crystalline borate phases within the geopolymer [25]. The XRD patterns of these crystalline phases, such as borax, sodium borate, tripotassium triborate,

and sodium borate hydrate, disappeared or their intensities decreased markedly as the Ca/Al ratio increased (Fig. 1). In other words, excessive addition of Ca(OH)<sub>2</sub> is presumed to have further facilitated the decomposition of physically immobilized BW, leading to the release of borate during leaching tests. While the addition of Ca(OH)<sub>2</sub> has an overall positive impact on the leaching resistance of B, it has been confirmed that adding an appropriate amount of Ca(OH)<sub>2</sub> is more effective than a simply increasing the Ca content.

688

689

690

691

692

693

694

695

696

697

698

699

700

701

702

703

704

705

706

707

708

709

710

A comprehensive understanding of the structural changes in waste form following the introduction of inorganic additives and the mechanisms that enhance the physicochemical performance is essential for the safe disposal of radioactive waste in underground facilities. In this study, the addition of Ca(OH)<sub>2</sub> was generally effective in improving the mechanical strength of geopolymer waste forms containing a high concentration of BW at 30 wt% and enhancing the resistance of B to long-term leaching. The geopolymer with a Ca/Al ratio of 1.0 exhibited a more pronounced indication of C-(A)-S-H gel formation. The scientific evidence supporting this observation was obtained through analyses involving XRD, solid-state MAS NMR, in-situ high-temperature XRD, and SEM/EDS. However, confirming the formation of C-(A)-S-H gel through these characterizations proved challenging in geopolymers with the lowest Ca(OH)<sub>2</sub> content, despite their notable improvements in compressive strength and leaching resistance. The overall research findings suggest that C-(A)-S-H gel was formed, but its quantitative amount was minimal, and atomic ordering was poor due to low Ca content. Geopolymer is a versatile binder material for immobilizing radioactive waste which is challenging to solidify/stabilize with cementitious waste forms; however, its stability and performance can vary depending on the physicochemical characteristics of the radioactive waste. Therefore, the use of chemical additives to enhance the durability of geopolymer waste

forms should be considered. The findings of this study indicate that the use of  $Ca(OH)_2$  as a chemical additive in the geopolymer waste form for radioactive waste management is advantageous. Improved durability and leaching resistance in the geopolymer waste form when  $Ca(OH)_2$  is added adequately was also demonstrated.

715

716

717

718

719

720

721

722

723

724

725

726

727

728

729

730

731

732

733

711

712

713

714

## 4. Conclusion

The physicochemical characteristics of geopolymer waste form were enhanced by adding Ca(OH)2, and structural changes were investigated. The crystalline borate phases partially dissolved, and C-(A)-S-H gel formation was confirmed by an increase in the Ca/Al ratio. The 7-day compressive strength increased approximately two to three times compared to the geopolymer waste form without Ca(OH)2, whereas it gradually decreased as the Ca/Al ratio increased. This is attributed to the excess Ca(OH)2 leading to the further dissolution of metakaolin and resulting in the fast setting of geopolymer. Simultaneously, the reduction of the protective layer on the surface of metakaolin by C-(A)-S-H gel formation led to the high viscosity and low workability of geopolymer paste. Meanwhile, added Ca(OH)2 led to a decrease in the chemical immobilization of BW. This is attributed to a reduction in reactive silicate caused by the formation of C-(A)-S-H gel. The characterizations, such as solid-state MAS NMR, thermal analysis, *in-situ* high-temperature XRD, and SEM/EDS revealed that the addition of Ca(OH)<sub>2</sub> resulted in the formation of a more extensive geopolymer gel-like structure, a compact microstructure, and participation in the geopolymerization reaction of Na released from BW. The Ca/Al ratio effective in improving the B leaching resistance was 0.25, which is consistent with the improved compressive strength results, and CFL decreased from 0.41 to 0.18. The 100-day average leachability index of B increased from 7.5 to 8.7. The leaching

mechanism of B shifted from surface wash-off to diffsuion. The partial dissolution of physically immobilized BW and the limited formation of the B-O-Si network contributed to this. These research findings demonstrate the advantage of adding proper amount of Ca(OH)<sub>2</sub> for enhancing the durability and leaching resistance of geopolymer waste forms.

#### 739

740

# Acknowledgement

- This work was supported by the Institute for Korea Spent Nuclear Fuel (iKSNF) and
- 742 Korea Foundation of Nuclear Safety (KOFONS) grant funded by the Korea Government
- 743 (Nuclear Safety and Security Commission, NSSC) (No. RS-2021-KN066120) and Nuclear
- Global Fellowship Program through KONICOF funded by the Ministry of Science and ICT
- 745 (Project No. 2022M2C7A1A03062813).

746

747

## References

- 748 [1] J.H. Kim, B.G. Ahn, H.Y. Kim, H.H. Park, A study on the Solidification of Borate Waste
- 749 using Cement, J. Korea Soc. Waste Manag., (1989) 137-142.
- 750 [2] H.J. Cho, D.M. Kim, J.K. Park, Study on Pre-treatment Method for Vitrification of
- Concentrated Wastes, J. Korea Soc. Waste Manag., 8 (2010) 221-227.
- 752 [3] B. Kim, J. Kang, Y. Shin, W. Um, Waste acceptance criteria testings of a phosphate-based
- 753 geopolymer waste form to immobilize radioactive borate waste, J. Nucl. Mater., 586 (2023)
- 754 154671. https://doi.org/10.1016/j.jnucmat.2023.154671
- 755 [4] M.Y. Park, A Study on the Optimization of Solidification Process for Radioactive Waste
- Not Suitable for Disposal by Pelletization, Chosun University, 2020.
- 757 [5] D.C. Tsang, L. Wang, Low Carbon Stabilization and Solidification of Hazardous Wastes,
- 758 Elsevier, 2021.
- 759 [6] M. Atkins, F. Glasser, Application of Portland cement-based materials to radioactive waste
- 760 immobilization, Waste Manag., 12 (1992) 105-131.
- 761 [7] F. Bart, C. Cau-di-Coumes, F. Frizon, S. Lorente, Cement-based materials for nuclear waste

- storage, Springer Science & Business Media, 2012.
- 763 [8] M. Davraz, The Effect of Boron Compound to Cement Hydration and Controllability of
- 764 this Effect, Acta Phys. Pol. A., 128 (2015) B26-B33. https://doi.org/
- 765 10.12693/APhysPolA.128.B-26
- 766 [9] A. Palomo, J.I.L. de la Fuente, Alkali-activated cementitous materials: Alternative matrices
- for the immobilisation of hazardous wastes Part I. Stabilisation of boron, Cem. Concr. Res.,
- 768 33 (2003) 281-288. https://doi.org/10.1016/S0008-8846(02)00963-8
- 769 [10] B. Kim, J. Lee, J. Kang, W. Um, Development of geopolymer waste form for
- immobilization of radioactive borate waste, J. Hazard. Mater., 419 (2021) 126402.
- 771 https://doi.org/10.1016/j.jhazmat.2021.126402
- 772 [11] J.B. Champenois, C.C.D. Coumes, A. Poulesquen, P. Le Bescop, D. Damidot, Beneficial
- use of a cell coupling rheometry, conductimetry, and calorimetry to investigate the early age
- 774 hydration of calcium sulfoaluminate cement, Rheol. Acta, 52 (2013) 177-187.
- 775 https://doi.org/10.1007/s00397-013-0675-9
- 776 [12] H.C. Lee, Y.H. Chang, Solidify Properties of Radiactive Waste using Parffin Wax, J.
- 777 Korean Ind. Eng. Chem., 17 (2006) 391-396.
- 778 [13] J. Sheng, K. Choi, M.J. Song, Vitrification of liquid waste from nuclear power plants, J.
- 779 Nucl. Mater., 297 (2001) 7-13.
- 780 [14] B. Kim, S. Lee, Review on characteristics of metakaolin-based geopolymer and fast setting,
- 781 J. Korean Ceram. Soc., 57 (2020) 368-377. https://doi.org/10.1007/s43207-020-00043-y
- 782 [15] Q. Tian, S. Nakama, K. Sasaki, Immobilization of cesium in fly ash-silica fume based
- geopolymers with different Si/Al molar ratios, Sci. Total Environ., 687 (2019) 1127-1137.
- 784 https://doi.org/10.1016/j.scitotenv.2019.06.095
- 785 [16] R.I. Chaerun, N. Soonthornwiphat, K. Toda, K. Kuroda, X.B. Niu, R. Kikuchi, T. Otake,

- Y. Elakneswaran, J.L. Provis, T. Sato, Retention mechanism of cesium in chabazite embedded
- 787 into metakaolin-based alkali activated materials, J. Hazard. Mater., 440 (2022) 129732.
- 788 https://doi.org/10.1016/j.jhazmat.2022.129732
- 789 [17] X. Ke, S.A. Bernal, T. Sato, J.L. Provis, Alkali aluminosilicate geopolymers as binders to
- encapsulate strontium-selective titanate ion-exchangers, Dalton Trans., 48 (2019) 12116-12126.
- 791 https://doi.org/10.1039/C9DT02108F
- 792 [18] Y. Shin, B. Kim, J. Kang, H.M. Ma, W. Um, Estimation of radionuclides leaching
- characteristics in different sized geopolymer waste forms with simulated spent ion-exchange
- resin, Nucl. Eng. Tech., 55 (2023) 3617-3627. https://doi.org/10.1016/j.net.2023.06.026
- 795 [19] V. Cuccia, C.B. Freire, A.C.Q. Ladeira, Radwaste oil immobilization in geopolymer after
- 796 non-destructive treatment, Prog. Nucl. Energy, 122 (2020) 103246.
- 797 https://doi.org/10.1016/j.pnucene.2020.103246
- 798 [20] V. Cantarel, F. Nouaille, A. Rooses, D. Lambertin, A. Poulesquen, F. Frizon,
- 799 Solidification/stabilisation of liquid oil waste in metakaolin-based geopolymer, J. Nucl. Mater.,
- 800 464 (2015) 16-19. https://doi.org/10.1016/j.jnucmat.2015.04.036
- 801 [21] E. Mossini, A. Santi, G. Magugliani, F. Galluccio, E. Macerata, M. Giola, D. Vadivel, D.
- 802 Dondi, D. Cori, P. Lotti, G.D. Gatta, M. Mariani, Pre-impregnation approach to encapsulate
- radioactive liquid organic waste in geopolymer, J. Nucl. Mater., 585 (2023) 154608.
- 804 https://doi.org/10.1016/j.jnucmat.2023.154608
- 805 [22] S. Watanabe, Y. Takahatake, H. Ogi, T. Osugi, T. Taniguchi, J. Sato, T. Arai, A. Kajinami,
- Decontamination and solidification treatment on spent liquid scintillation cocktail, J. Nucl.
- 807 Mater., 585 (2023) 154610. https://doi.org/10.1016/j.jnucmat.2023.154610
- 808 [23] N. Kozai, J. Sato, T. Osugi, I. Shimoyama, Y. Sekine, F. Sakamoto, T. Ohnuki, Sewage
- sludge ash contaminated with radiocesium: Solidification with alkaline-reacted metakaolinite

- 810 (geopolymer) and Portland cement, J. Hazard. Mater., 416 (2021) 125965.
- 811 https://doi.org/10.1016/j.jhazmat.2021.125965
- 812 [24] J.X. Wang, L. Han, Z. Liu, D.M. Wang, Setting controlling of lithium slag-based
- 813 geopolymer by activator and sodium tetraborate as a retarder and its effects on mortar
- 814 properties, Cem. Concr. Compos., 110 (2020) 103598.
- 815 https://doi.org/10.1016/j.cemconcomp.2020.103598
- 816 [25] B. Kim, J. Kang, Y. Shin, T.M. Yeo, J. Heo, W. Um, Effect of Si/Al molar ratio and curing
- 817 temperatures on the immobilization of radioactive borate waste in metakaolin-based
- 818 geopolymer waste form, J. Hazard. Mater., 458 (2023) 131884.
- 819 https://doi.org/10.1016/j.jhazmat.2023.131884
- 820 [26] K.M.L. Alventosa, B. Wild, C.E. White, The effects of calcium hydroxide and activator
- chemistry on alkali-activated metakaolin pastes exposed to high temperatures, Cem. Concr.
- 822 Res., 154 (2022) 106742. https://doi.org/10.1016/j.cemconres.2022.106742
- 823 [27] X. Chen, A. Sutrisno, L.Y. Zhu, L.J. Struble, Setting and nanostructural evolution of
- 824 metakaolin geopolymer, J. Am. Ceram. Soc., 100 (2017) 2285-2295.
- 825 https://doi.org/10.1111/jace.14641
- 826 [28] B. Kim, S. Lee, C.M. Chon, S. Cho, Setting Behavior and Phase Evolution on Heat
- Treatment of Metakaolin-Based Geopolymers Containing Calcium Hydroxide, Materials, 15
- 828 (2022) 194. https://doi.org/10.3390/ma15010194
- 829 [29] American National Standard, Measurement of the Leachability of Solidified LowLevel
- Radioactive Wastes by a Short-Term Test Procedure, 1986. ANSI/ANS-16.1-.
- 831 [30] B. Walkley, S.J. Page, G.J. Rees, J.L. Provis, J.V. Hanna, Nanostructure of CaO-(Na2O)-
- Al2O3-SiO2-H2O gels revealed by multinuclear solid-state magic angle spinning and multiple
- quantum magic angle spinning nuclear magnetic resonance spectroscopy, J. Phys. Chem. C,

- 834 124 (2019) 1681-1694. https://doi.org/10.1021/acs.jpcc.9b10133
- 835 [31] R.Z. Si, S.C. Guo, Q.L. Dai, Influence of calcium content on the atomic structure and
- phase formation of alkali-activated cement binder, J. Am. Ceram. Soc., 102 (2019) 1479-1494.
- 837 https://doi.org/10.1111/jace.15968
- 838 [32] X.B. Niu, Y. Elakneswaran, R.I. Chaerun, C.W. Fang, N. Hiroyoshi, J.L. Provis, T. Sato,
- Development of metakaolin-based geopolymer for selenium oxyanions uptake through in-situ
- 840 ettringite formation, Sep. Purif. Technol., 324 (2023) 124530.
- 841 https://doi.org/10.1016/j.seppur.2023.124530
- 842 [33] S. Ortaboy, J. Li, G. Geng, R.J. Myers, P.J. Monteiro, R. Maboudian, C. Carraro, Effects
- of CO 2 and temperature on the structure and chemistry of C–(A–) S–H investigated by Raman
- spectroscopy, RSC advances, 7 (2017) 48925-48933. https://doi.org/10.1039/C7RA07266J
- 845 [34] B. Walkley, X.Y. Ke, J.L. Provis, S.A. Bernal, Activator Anion Influences the
- Nanostructure of Alkali-Activated Slag Cements, J. Phys. Chem. C, 125 (2021) 20727-20739.
- 847 https://doi.org/10.1021/acs.jpcc.1c07328
- 848 [35] S.H. Hyun, T.M. Yeo, H.M. Ha, J.W. Cho, Structural evidence of mixed alkali effect for
- 849 aluminoborosilicate glasses, J. Mol. Liq., 347 (2022) 118319.
- 850 https://doi.org/10.1016/j.molliq.2021.118319
- 851 [36] X. Chen, A. Sutrisno, L.J. Struble, Effects of calcium on setting mechanism of metakaolin-
- 852 based geopolymer, J. Am. Ceram. Soc., 101 (2018) 957-968.
- 853 https://doi.org/10.1111/jace.15249
- 854 [37] B. Walkley, R. San Nicolas, M.A. Sani, G.J. Rees, J.V. Hanna, J.S.J. van Deventer, J.L.
- Provis, Phase evolution of C-(N)-A-S-H/N-A-S-H gel blends investigated via alkali-activation
- of synthetic calcium aluminosilicate precursors, Cem. Con. Res., 89 (2016) 120-135.
- 857 https://doi.org/10.1016/j.cemconres.2016.08.010

- 858 [38] A. Aboulayt, M. Riahi, M.O. Touhami, H. Hannache, M. Gomina, R. Moussa, Properties
- of metakaolin based geopolymer incorporating calcium carbonate, Adv. Powder Technol., 28
- 860 (2017) 2393-2401. https://doi.org/10.1016/j.apt.2017.06.022
- 861 [39] C.K. Yip, J.L. Provis, G.C. Lukey, J.S.J. van Deventer, Carbonate mineral addition to
- metakaolin-based geopolymers, Cem. Concr. Compos., 30 (2008) 979-985.
- 863 https://doi.org/10.1016/j.cemconcomp.2008.07.004
- 864 [40] J. Temuujin, A. van Riessen, R. Williams, Influence of calcium compounds on the
- mechanical properties of fly ash geopolymer pastes, J. Hazard. Mater., 167 (2009) 82-88.
- 866 https://doi.org/10.1016/j.jhazmat.2008.12.121
- 867 [41] B. Ma, Y. Luo, L.Z. Zhou, Z.Y. Shao, R.H. Liang, J. Fu, J.Q. Wang, J. Zang, Y.Y. Hu, L.M.
- Wang, The influence of calcium hydroxide on the performance of MK-based geopolymer,
- 869 Constr. Build. Mater., 329 (2022) 127224. https://doi.org/10.1016/j.conbuildmat.2022.127224
- 870 [42] S.K. Nath, S. Maitra, S. Mukherjee, S. Kumar, Microstructural and morphological
- evolution of fly ash based geopolymers, Constr. Build. Mater., 111 (2016) 758-765.
- 872 https://doi.org/10.1016/j.conbuildmat.2016.02.106
- 873 [43] P. Sturm, G.J.G. Gluth, S. Simon, H.J.H. Brouwers, H.C. Kühne, The effect of heat
- 874 treatment on the mechanical and structural properties of one-part geopolymer-zeolite
- composites, Thermochim. Acta, 635 (2016) 41-58. https://doi.org/10.1016/j.tca.2016.04.015
- 876 [44] P.G. He, D.C. Jia, M.R. Wang, Y. Zhou, Thermal evolution and crystallization kinetics of
- potassium-based geopolymer, Ceram. Int., 37 (2011) 59-63.
- 878 https://doi.org/10.1016/j.ceramint.2010.08.008
- 879 [45] E. Kamseu, A. Rizzuti, C. Leonelli, D. Perera, Enhanced thermal stability in K 2 O-
- metakaolin-based geopolymer concretes by Al2O3 and SiO2 fillers addition, J. Mater. Sci., 45
- 881 (2010) 1715-1724. https://doi.org/10.1007/s10853-009-4108-1

- 882 [46] P. Duxson, G.C. Lukey, F. Separovic, J.S.J. van Deventer, Effect of alkali cations on
- aluminum incorporation in geopolymeric gels, Ind. Eng. Chem. Res., 44 (2005) 832-839.
- 884 https://doi.org/10.1021/ie0494216
- 885 [47] B. Walkley, G.J. Rees, R. San Nicolas, J.S. van Deventer, J.V. Hanna, J.L. Provis, New
- structural model of hydrous sodium aluminosilicate gels and the role of charge-balancing extra-
- 887 framework Al, J. Phys. Chem. C, 122 (2018) 5673-5685.
- 888 https://doi.org/10.1021/acs.jpcc.8b00259
- 889 [48] P. Duxson, J.L. Provis, G.C. Lukey, S.W. Mallicoat, W.M. Kriven, J.S.J. van Deventer,
- 890 Understanding the relationship between geopolymer composition, microstructure and
- mechanical properties, Colloids Surf. A: Physicochem. Eng. Asp., 269 (2005) 47-58.
- 892 https://doi.org/10.1016/j.colsurfa.2005.06.060
- 893 [49] A.E. Alexander, A.P. Shashikala, Studies on the microstructure and durability
- characteristics of ambient cured FA-GGBS based geopolymer mortar, Constr. Build. Mater.,
- 895 347 (2022) 128538. https://doi.org/10.1016/j.conbuildmat.2022.128538
- 896 [50] X. Xue, Y.L. Liu, J.G. Dai, C.S. Poon, W.D. Zhang, P. Zhang, Inhibiting efflorescence
- formation on fly ash-based geopolymer via silane surface modification, Cem. Concr. Compos.,
- 898 94 (2018) 43-52. https://doi.org/10.1016/j.cemconcomp.2018.08.013
- 899 [51] B. Walkley, R. San Nicolas, M.A. Sani, J.D. Gehman, J.S.J. van Deventer, J.L. Provis,
- 900 Synthesis of stoichiometrically controlled reactive aluminosilicate and calcium-aluminosilicate
- 901 powders, Powder Technol., 297 (2016) 17-33. https://doi.org/10.1016/j.powtec.2016.04.006